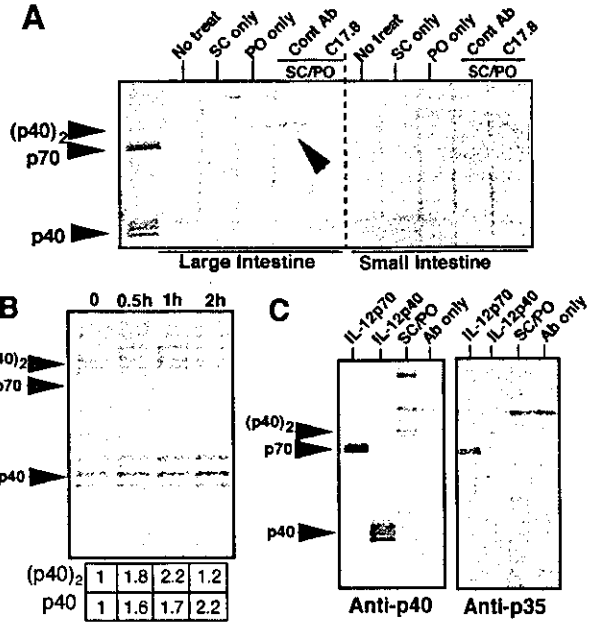

Figure 2. Induction of IL-12p40 homodimer in the large but not small intestine of diarrhea-induced mice. Large and small intestinal tissue extracts were subjected to immunopreciptation and Western blotting analysis using anti-IL-12p40 (C17.8) mAb under non-reducing conditions (**A**). The captions above the figure indicate the experimental mouse group receiving different *in vivo* treatments. Thus, the samples were obtained from SC/PO mice treated with C17.8 or control antibodies. Further, the samples were isolated from mice treated with PO only, SC only, or non-treated mice. The **arrow** points to IL-12p40 homodimer expression in the large intestine of diarrhea-induced mice. The data represent four independent experiments. In **B**, at the indicated times after oral administration of OVA, large intestinal tissue extracts isolated from diarrhea-induced mice were assayed for IL-12p40 by the same method as in **A**. In **C**, the large intestinal tissue extracts of diarrhea-induced mice were subjected to Western blotting with anti-IL-12p35 Ab as well as anti-IL-12p40. IL-12p70 protein was used as a positive control for the IL-12p35 detection system. As negative control, immunoprecipitation was performed without the tissue specimens (Ab only). The data represent three different experiments.

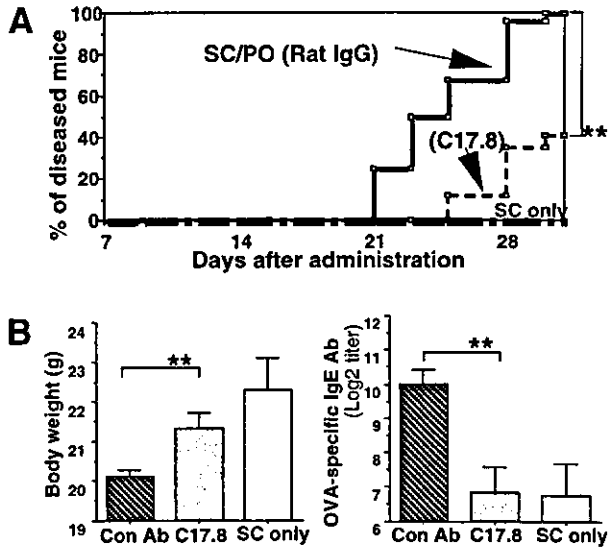

Figure 3. Inhibition of allergic diarrhea disease by the treatment with anti-IL-12p40 mAb. In **A**, anti-IL-12p40 mAb (C17.8) treatment (**thin dashed line**) delayed the development of allergic diarrhea when compared with the rat IgG-treated group (**solid line**). Statistical differences were determined by Wilcoxon rank-sum test and are indicated by **, $P < 0.01$. Mice with SC only were used as controls (**thick dashed line**). In **B**, **left**, body weight was recovered in allergic diarrhea mice treated with anti-IL-12p40 mAb (C17.8). In **B**, **right**, OVA-specific IgE Abs were reduced in the serum of allergic diarrhea mice treated with anti-IL-12p40 mAb (C17.8). The data are expressed as the mean of ± SE and are representative of five independent experiments. Statistical differences between anti-IL-12p40 mAb and control rat IgG-treated mice are indicated as **, $P < 0.01$.

ble for the production of IL-12p40 at the disease site of OVA-induced allergic diarrhea.

The Western blotting method was adopted for the examination of IL-12 p40 expression in the small and large intestinal tissue extracts from OVA-induced allergic diarrhea mice within 1 to 2 hours after the last oral challenge. In the large intestine of diarrhea-induced mice, the 80kD form of IL-12 predominated clearly demonstrating the presence of IL-12p40 homodimer but not 70kD IL-12 heterodimer, in contrast to the environment observed in the large intestine of control mice or the small intestine of mice with/without diarrhea (Figure 2A). The multiple bands of p40 and p80 are the result of glycosylation heterogenity.[15] We thus analyzed three bands of p40 and three bands of p80 as specific bands. In the case of spleen, IL-12p40 was detected in control, healthy mice. The levels of IL-12p40 did not change after development of allergic diarrhea (data not shown). To examine the kinetics of the response, we next assessed the time course of IL-12p40 expression in the large intestine of the diarrhea-induced mice. The expression of IL-12p40 or p80 in the large intestine peaked between 1 and 2 hours after the last oral challenge, at the same time that severe symptoms of OVA-induced allergic diarrhea were observed (Figure 2B). These data suggest that there is an intimate relationship between the development of diarrhea and the expression of IL-12p40 in the large intestine.

To further confirm the expression of IL-12p80 or p40 instead of the p70 form, the protein extracts from the large intestine of the diarrhea-induced mice were immunoprecipitated with anti-IL-12p40 mAb and then Western blotting was performed using anti-IL-12p35 mAb. No molecular bands corresponding to IL-12p70 proteins were detected in the large intestine of diarrhea-induced mice, while predominant IL-12p40 protein was detected (Figure 2C). The large molecular weight band above the p70 and p80 bands was non-specific and was caused by the nature of antibody used in the immunoprecipitation, since the large molecular weight band was also seen following immunoprecipitation in the absence of tissue specimens (Ab only in Figure 2C). These results indicate that the secretion of IL-12p40, but not IL-12p70, in the large intestine is critically important in the development of OVA-induced allergic diarrhea.

Anti-IL-12p40 Treatment Reduced the Symptoms of Allergic Diarrhea

Inasmuch as the preferential localization of IL-12p40 was observed in mice with allergic diarrhea, we next performed a neutralization experiment using anti-IL-12p40 mAb (C17.8). We observed a significant delay in the onset of diarrhea and reduced the frequency of diarrhea to 40% by treatment with anti-IL-12p40 mAb (Figure 3A). Obvious body weight loss was seen in control Ig-treated

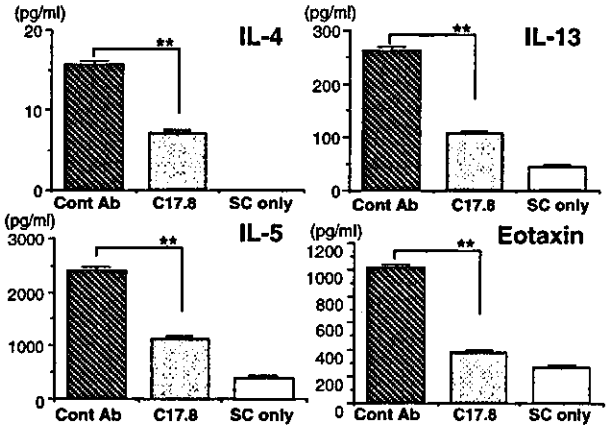

Figure 4. *In vivo* treatment with anti-IL-12p40 (C17.8) reduced the predominant antigen-specific Th2 type responses by large intestinal mononuclear cells isolated from diarrhea-induced mice. The mononuclear cells isolated from the large intestine (1.5×10^5 cells/well) were cultured with OVA (1 mg/ml) for 3 days. Culture supernatants were harvested and then assayed for IL-4, IL-13, IL-5, and eotaxin by ELISA assay. These data are expressed as the mean ± SE and are representative of three independent experiments. The statistical differences between anti-IL-12p40 mAb and control antibody treated mice are indicated as **, $P < 0.01$.

diarrhea mice, while treatment with anti-IL-12p40 mAb resulted in partial recovery from body weight loss (Figure 3B, left). In addition, high levels of OVA-specific IgE Abs were detected in the serum of diarrhea-induced mice treated with control Ab, whereas the mice treated with anti-IL-12p40 mAb showed low levels of OVA-specific IgE Abs (Figure 3B, right). These results indicate that treatment with anti-IL-12p40 mAb alters the environment from a disease-inducing one to one fastening recovery in OVA-induced allergic diarrhea.

Suppression of Intestinal Th2-Type Cytokine by Anti-IL-12p40 Treatment

To confirm decreased Th2-type responses in the large intestine after anti-IL-12p40 mAb treatment, we next examined antigen-induced cytokine production by the large intestinal mononuclear cells. Interestingly, the anti-IL-12p40 treatment resulted in decreased levels of OVA-induced Th2 cytokine synthesis including those of IL-4, IL-5, and IL-13 (Figure 4). Production levels of the Th2 cytokines were comparable to those of control mice without allergic diarrhea (SC only). In contrast to the alterations observed in OVA-induced Th2 cytokine synthesis, there was no difference in the level of IFN-γ production between the mice treated with anti-IL-12p40 mAb and control IgG (data not shown). We further confirmed that IL-4 producing cells were $CD4^+$ Th2 cells by intracellular staining (data not shown).

Finally, the level of eotaxin, a well-known chemokine for eosinophil recruitment in allergic disease,[30] was also examined, since our previous study demonstrated that the frequency of eosinophils was increased in the large intestine of allergic diarrhea mice.[1] Likewise, the level of eotaxin could also be presumed to be increased in the large intestine of allergic diarrhea mice (Figure 4). Interestingly however, the level of eotaxin synthesis was significantly decreased by the treatment with anti-IL-12p40 mAb (Figure 4). These results indicate that anti-IL-12p40 mAb inhibited the immunopathological Th2 cytokine environment of the large intestine in allergic diarrhea mice. Thus, an interesting scenario could be the presence of high levels of IL-12p40 monomer and/or homodimers instead of IL-12p70 in the disease site of OVA-induced allergic diarrhea mice. Therefore, treatment with anti-IL-12p40 mAb might result in the inhibition of Th2-type responses in the large intestine of allergic disease mice.

A

Immunization	Mice	OVA-induced diarrhea (%)
SC / PO	WT	100
	IL-12p40 KO	0
SC only	WT	0

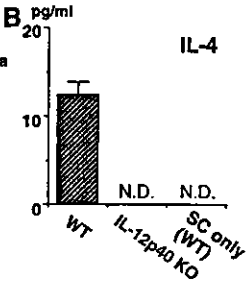

Figure 5. Suppression of allergic diarrhea development in IL-12p40 KO mice. In **A**, the incidence of allergic diarrhea was reduced in the IL-12p40 KO mice when compared with wild-type mice immunized subcutaneously and then given OVA repeatedly by the oral route (SC/PO). In **B**, the large intestinal LP mononuclear cells from IL-12p40 KO mice did not produce IL-4. Mononuclear cells isolated from the large intestine were restimulated with OVA for the assessment of IL-4 synthesis as described in Figure 4A. The data are expressed as the mean ± SE and represent three different experiments.

IL-12p40-Deficient Mice Do Not Develop Allergic Diarrhea

To directly confirm the pathological role of IL-12p40 in the development of allergic diarrhea, IL-12p40 knockout (KO) mice were used. IL-12p40 KO mice did not develop the allergic diarrhea completely (Figure 5A). OVA-induced IL-4 production by large intestinal LP mononuclear cells was not detected in IL-12p40 mice (Figure 5B). The levels of other Th2-type cytokines (IL-5 and IL-10) were also reduced in IL-12p40 KO mice (data not shown). Taken together, these results clearly show that IL-12p40 plays an important role in the development of this large intestinal allergic disease.

Discussion

Our present findings provide new, strong evidence for an immunopathological role for locally produced IL-12p40 in the development of OVA-induced allergic diarrhea. Here we demonstrate the high expression of IL-12p40, without IL-12p35, in the large intestine but not in the small intestine of mice with allergic diarrhea. These IL-12p40 were locally produced by large intestinal MØ, DC, and epithelial cells. Based on our knowledge, this is the first demonstration of the presence of IL-12p40 in the selected part of the intestinal tract (eg, large intestine) in mice with allergic diarrhea. Although IL-12 is thought to drive the Th1-dominant environment,[31] our present findings provide additional supportive evidence that IL-12p40 contributes to the generation of a Th2-dominant environ-

ment.[18,19] It should be noted that our results directly demonstrate the *in vivo* immunopathological contribution of locally produced mucosal IL-12p40 to the development of OVA-induced diarrhea. Thus, the anti-IL-12p40 treatment reduced the incidence of OVA-induced allergic diarrhea. An attractive explanation would be that large intestinal MØs and DCs as well as epithelial cells contribute to the development of pathological Th2-dominant responses by the production of IL-12p40 in OVA-induced allergic diarrhea. Thus, the administration of anti-IL-12p40 resulted in the inhibition of the locally produced, mucosal IL-12p40-created, pathological Th2 condition, leading to the reduction of disease development.

Our present and previous results clearly show that large intestinal antigen-specific Th cells produce high levels of Th2 cytokine in OVA-induced allergic diarrhea.[1] The presence of monomeric or dimeric forms of IL-12p40, behaving as an antagonist to IL-12p70, is an additional contributing factor for the creation of a dominant pathological Th2 environment. Thus, the severe symptoms of allergic diarrhea were reduced by treatment with anti-IL-12p40 mAb, since the production of Th2 cytokines was significantly decreased in the large intestine. Overall, IL-12p40-supported, Th2-type cytokine synthesis plays a critical and pathological role in the induction of allergic reactions in large intestinal tissues. Although we do not have any specific explanation for the generation of IL-12p40 at the disease site, one possibility could be antigen overload in the intestinal tract. Our previous study demonstrated that oral administration of high doses of OVA induced Th2-mediated allergic diarrhea in systematically pre-sensitized BALB/c mice.[1] In contrast, low doses of oral OVA failed to induce allergic diarrhea. It was also shown that high doses of OVA peptide increased the numbers of naive $CD4^+$ T cells with Th2-like phenotype, which in turn produced dramatically large amounts of IL-4.[32] Therefore, high doses of oral antigen may create an immunological environment favoring Th2 cell development. To support this view, it has also been shown that high doses of oral antigen preferentially inhibit IFN-γ-producing Th1-type cells.[1] Further, the dose of antigen can determine whether Th1- or Th2-type cells are generated by antigen-presenting cells including DC.[33] Taken together, these findings allow us to postulate that an overload of oral antigen may direct mucosal antigen-presenting cells, including DC and MØ, and epithelial cells, to produce monomeric or dimeric forms of IL-12p40 instead of IL-12p70.

IL-12 has been considered as an inhibitory factor for allergic responses induced by preferential Th2-cytokine production. Indeed, endogenous rIL-12 decreased IgE levels and Th2 cytokine production induced by allergic reaction.[34] In contrast, IL-12 has also been shown to be involved in the pathological phase of mucosa-associated allergic diseases of the respiratory tract. In the murine asthma model, IL-12 contributed to the recruitment of eosinophils into the respiratory tract via the induction of VCAM-1 on local vascular epithelial cells.[35] Thus, the deletion of the IL-12 gene (p40) resulted in a substantial reduction in the airway recruitment of eosinophils and in the expression of VCAM-1 when compared with wild-type mice exhibiting an asthma-like reaction induced by systemic sensitization followed by nasal OVA.[36] In addition, selective overexpression of IL-12p40 was noted in airway epithelial cells and bronchoalveolar lavage fluids of patients with asthma.[20] Our present findings also demonstrate that the locally produced p40 form of IL-12 was associated with the development of OVA-induced allergic diarrhea. Thus, IL-12p40 was preferentially expressed only in the large intestine of allergic diarrhea mice. In addition to these results generated through the characterization of an asthma model, our present finding suggests a critical role for IL-12, especially that of p40-associated molecules, for the development of allergic diseases including asthma and food allergy.

The treatment with anti-IL-12p40 mAbs effectively reduced the incidence as well as the severity of allergic diarrhea, an effect most likely due to an alteration in the dominant immunopathological Th2-type response to a Th1-type environment. To support this view, locally overexpressed IL-12p40 may compete with the well-known Th1 promoter IL-12p70 and IL-23 (p40/p19).[37–39] To this end, it has been shown that endogenous IL-12p40 can overcome the Th1-promoting activity of IL-12p70 and/or IL-23.[18] In this regard, our recent and separate study showed that IL-23p19-specific mRNA expression was not detected in either diseased or healthy BALB/c mouse groups (data not shown). The results suggest that IL-23 dose not play an important role in the development of our diarrhea model. Therefore, treatment with anti-IL-12p40 antibody likely eliminated the antagonistic effect of IL-12p40 at the local site, perhaps leading to the creation of an IL-12p70 environment for the initiation of down-regulation of Th2 responses. An alternative explanation would be that anti-IL-12p40 mAb used in this experiment may possess a higher affinity for the monomeric or dimeric form of IL-12 than for the IL-12p70 heterodimer. Although our emphasis has been on the inhibitory effects of anti-IL-12p40 mAb for the prevention of allergic diarrhea, one must accept the fact that complete prevention of disease development was never achieved through use of mAbs. A possible explanation for this finding could be that anti-IL-12p40 mAb inhibited Th1 induction of IL-12p70 in addition to IL-12p40. Thus, this alteration of a Th2 dominant environment and shift to one of a Th1-type may partially occur in the large intestine of mice with allergic diarrhea. To support this possibility, the mAb used in these experiments has been shown to neutralize IL-12p70 in addition to IL-12p40.[13,14] In addition, the experiments using IL-12p40 KO mice suggest that the absence of IL-12p40 results in a complete failure to develop allergic diarrhea. It clearly shows that IL-12p40 play a critical role in the development of this disease. However, one alternative and simple expectation would be that an IL-12p40 deficiency may lead to the creation of Th2 environment due to the lack of Th1 inducing IL-12p70. Thus, it may lead to the more susceptible condition for the development of Th2-mediated diarrhea. Although we do not have any specific data to negate the latter possibility, one possible explanation would be that the deficiency of IL-12p70 formation in IL-12p40 KO mice lead to the lack of ability to active antigen presenting cells. IL-12p70 deficiency may

result in the absence of induction antigen-specific T cell response including the pathological Th2-type cells. It has been shown that IL-12 or IL-12-induced IFNγ can directly activate antigen presenting cells.[40] To address the issue, a series of interesting experiment would be the adaptive transfer of large intestinal MØ, DC, and epithelial cells into IL-12p40 and/or p35 KO mice. These experiments are, of course, planned for our future study.

Recently, it has been suggested that IL-12 is also one of the key cytokines for the regulation of the intestinal immune response.[41] Mouse IL-12p40 is produced as monomer and homodimer five to ninety times as frequently as IL-12p70 *in vivo* and *in vitro*,[40,42] implying the existence of additional immunological roles for IL-12p40. An interesting possibility would be that excess production of the monomeric and/or the homodimeric form of IL-12p40 could be a key contributing factor to the maintenance of immunological homeostasis at the mucosal compartment. Interestingly, our present findings demonstrate that over-expression of IL-12p40 occurred only in the large but not the small intestine following oral exposure to high doses of protein antigen. At the present time, we cannot offer any specific explanation for this distinct localization of IL-12p40. However, an interesting possibility would be that the expression of negative regulators for IL-12, including sCD40L and IL-10R,[14,43] could differ between the small and large intestine. To support this possibility, epithelial cells have been shown to express CD40 and IL-10R.[34,44] Since the large intestinal tract is continuously exposed to overloaded microflora, the level of co-stimulatory molecule expression such as CD40 by large intestinal epithelial cells could be lower to avoid unnecessary inflammatory responses. Thus, the large intestinal tract may form an immunological environment favoring the generation of IL-12p40. This interesting possibility is currently being tested in our laboratory.

In summary, our results demonstrated that locally produced IL-12p40 contribute to the Th2 cell generation of pathological polarization in the large intestine of OVA-induced allergic diarrhea. This study provides the first evidence for the association of over-expressed IL-12p40 from intestinal epithelial cells, DC and MØ, in the development of allergic diarrhea. Thus, the application of anti-IL-12p40 mAb resulted in the reduction of disease incidence and severity. Further, the disease development was completely eliminated in the deletion of IL-12p40 gene. Taken together, our studies provide an opportunity to consider that anti-IL-12p40 mAbs may be an alternative therapeutical regimen for the control of allergic intestinal disease.

Acknowledgments

We thank members of the Mucosal Immunology Group at Osaka University, The University of Tokyo and The University of Alabama at Birmingham, Immunobiology Vaccine Center for their helpful comments, Dr. Kimberly K. McGhee for editorial help, and Ms. Kelly Stinson and Ms. Sheila Turner for their help in the preparation of this manuscript.

References

1. Kweon MN, Yamamoto M, Kajiki M, Takahashi I, Kiyono H: Systemically derived large intestinal CD4+ Th2 cells play a central role in STAT6-mediated allergic diarrhea. J Clin Invest 2000, 106:199–206
2. Hogan SP, Mishra A, Brandt EB, Royalty MP, Pope SM, Zimmermann N, Foster PS, Rothenberg ME: A pathological function for eotaxin and eosinophils in eosinophilic gastrointestinal inflammation. Nat Immunol 2001, 2:353–360
3. Mishra A, Hogan SP, Brandt EB, Rothenberg ME: Peyer's patch eosinophils: identification, characterization, and regulation by mucosal allergen exposure, interleukin-5, and eotaxin. Blood 2000, 96: 1538–1544
4. Sampath D, Castro M, Look DC, Holtzman MJ: Constitutive activation of an epithelial signal transducer and activator of transcription (STAT) pathway in asthma. J Clin Invest 1999, 103:1353–1361
5. Shirakawa T, Enomoto T, Shimazu S, Hopkin JM: The inverse association between tuberculin responses and atopic disorder. Science 1997, 275:77–79
6. Das J, Chen CH, Yang L, Cohn L, Ray P, Ray A: A critical role for NF-κB in GATA3 expression and TH2 differentiation in allergic airway inflammation. Nat Immunol 2001, 2:45–50
7. Finotto S, Neurath MF, Glickman JN, Qin S, Lehr HA, Green FH, Ackerman K, Haley K, Galle PR, Szabo SJ, Drazen JM, De Sanctis GT, Glimcher LH: Development of spontaneous airway changes consistent with human asthma in mice lacking T-bet. Science 2002, 295:336–338
8. Spergel JM, Mizoguchi E, Oettgen H, Bhan AK, Geha RS: Roles of TH1 and TH2 cytokines in a murine model of allergic dermatitis. J Clin Invest 1999, 103:1103–1111
9. Korsgren M, Persson CG, Sundler F, Bjerke T, Hansson T, Chambers BJ, Hong S, Van Kaer L, Ljunggren HG, Korsgren O: Natural killer cells determine development of allergen-induced eosinophilic airway inflammation in mice. J Exp Med 1999, 189:553–562
10. Rodriguez-Sosa M, Satoskar AR, Calderon R, Gomez-Garcia L, Saavedra R, Bojalil R, Terrazas LI: Chronic helminth infection induces alternatively activated macrophages expressing high levels of CCR5 with low interleukin-12 production and Th2-biasing ability. Infect Immun 2002, 70:3656–3664
11. Jankovic D, Liu Z, Gause WC: Th1- and Th2-cell commitment during infectious disease: asymmetry in divergent pathways. Trends Immunol 2001, 22:450–457
12. Yoshimoto T, Kojima K, Funakoshi T, Endo Y, Fujita T, Nariuchi H: Molecular cloning and characterization of murine IL-12 genes. J Immunol 1996, 156:1082–1088
13. Hino A, Nariuchi H: Negative feedback mechanism suppresses interleukin-12 production by antigen-presenting cells interacting with T helper 2 cells. Eur J Immunol 1996, 26:623–628
14. Hino A, Igarashi O, Tagawa YI, Iwakura Y, Nariuchi H: Interferon-γ priming is not critical for IL-12 production of murine spleen cells. Cytokine 2000, 12:12–20
15. Heinzel FP, Hujer AM, Ahmed FN, Rerko RM: In vivo production and function of IL-12 p40 homodimers. J Immunol 1997, 158:4381–4388
16. Wang X, Wilkinson VL, Podlaski FJ, Wu C, Stern AS, Presky DH, Magram J: Characterization of mouse interleukin-12 p40 homodimer binding to the interleukin-12 receptor subunits. Eur J Immunol 1999, 29:2007–2013
17. Ling P, Gately MK, Gubler U, Stern AS, Lin P, Hollfelder K, Su C, Pan YC, Hakimi J: Human IL-12 p40 homodimer binds to the IL-12 receptor but does not mediate biologic activity. J Immunol 1995, 154:116–127
18. Piccotti JR, Chan SY, Li K, Eichwald EJ, Bishop DK: Differential effects of IL-12 receptor blockade with IL-12 p40 homodimer on the induction of CD4+ and CD8+ IFN-γ-producing cells. J Immunol 1997, 158:643–648
19. Yoshimoto T, Wang CR, Yoneto T, Waki S, Sunaga S, Komagata Y, Mitsuyama M, Miyazaki J, Nariuchi H: Reduced T helper 1 responses in IL-12 p40 transgenic mice. J Immunol 1998, 160:588–594
20. Walter MJ, Kajiwara N, Karanja P, Castro M, Holtzman MJ: Interleukin 12 p40 production by barrier epithelial cells during airway inflammation. J Exp Med 2001, 193:339–351
21. Hakonarson H, Maskeri N, Carter C, Grunstein MM: Regulation of TH1- and TH2-type cytokine expression and action in atopic asth-

matic sensitized airway smooth muscle. J Clin Invest 1999, 103:1077–1087
22. Wysocka M, Kubin M, Vieira LQ, Ozmen L, Garotta G, Scott P, Trinchieri G: Interleukin-12 is required for interferon-γ production and lethality in lipopolysaccharide-induced shock in mice. Eur J Immunol 1995, 25:672–676
23. Fujihira K, Nagata M, Moriyama H, Yasuda H, Arisawa K, Nakayama M, Maeda S, Kasuga M, Okumura K, Yagita H, Yokono K: Suppression and acceleration of autoimmune diabetes by neutralization of endogenous interleukin-12 in NOD mice. Diabetes 2000, 49:1998–2006
24. Fujihashi K, McGhee JR, Kweon MN, Cooper MD, Tonegawa S, Takahashi I, Hiroi T, Mestecky J, Kiyono H: γ/δ T cell-deficient mice have impaired mucosal immunoglobulin A responses. J Exp Med 1996, 183:1929–1935
25. Kweon MN, Fujihashi K, VanCott JL, Higuchi K, Yamamoto M, McGhee JR, Kiyono H: Lack of orally induced systemic unresponsiveness in IFN-γ knockout mice. J Immunol 1998, 160:1687–1693
26. Li L, Sad S, Kagi D, Mosmann TR: CD8Tc1 and Tc2 cells secrete distinct cytokine patterns in vitro and in vivo but induce similar inflammatory reactions. J Immunol 1997, 158:4152–4161
27. Stordeur P, Zhou L, Byl B, Brohet F, Burny W, de Groote D, van der Poll T, Goldman M: Immune monitoring in whole blood using real-time PCR. J Immunol Methods 2003, 276:69–77
28. Kinoshita N, Hiroi T, Ohta N, Fukuyama S, Park EJ, Kiyono H: Autocrine IL-15 mediates intestinal epithelial cell death via the activation of neighboring intraepithelial NK cells. J Immunol 2002, 169:6187–6192
29. Romijn HJ, van Uum JF, Breedijk I, Emmering J, Radu I, Pool CW: Double immunolabeling of neuropeptides in the human hypothalamus as analyzed by confocal laser scanning fluorescence microscopy. J Histochem Cytochem 1999, 47:229–236
30. Cuvelier SL, Patel KD: Shear-dependent eosinophil transmigration on interleukin 4-stimulated endothelial cells: a role for endothelium-associated eotaxin-3. J Exp Med 2001, 194:1699–1709
31. Trinchieri G: Interleukin-12: a cytokine produced by antigen-presenting cells with immunoregulatory functions in the generation of T-helper cells type 1 and cytotoxic lymphocytes. Blood 1994, 84:4008–4027
32. Hosken NA, Shibuya K, Heath AW, Murphy KM, O'Garra A: The effect of antigen dose on CD4+ T helper cell phenotype development in a T cell receptor-α β-transgenic model. J Exp Med 1995, 182:1579–1584
33. Ruedl C, Bachmman FB, Kopf M: The antigen dose determined T helper subset development by regulation of CD40 ligand. Eur J Immunol 2000, 30:2056–2064
34. Gavett SH, O'Hearn DJ, Li X, Huang SK, Finkelman FD, Wills-Karp M: Interleukin 12 inhibits antigen-induced airway hyper-responsiveness, inflammation, and Th2 cytokine expression in mice. J Exp Med 1995, 182:1527–1536
35. Kaminuma O, Fujimura H, Fushimi K, Nakata A, Sakai A, Chishima S, Ogawa K, Kikuchi M, Kikkawa H, Akiyama K, Mori A: Dynamics of antigen-specific helper T cells at the initiation of airway eosinophilic inflammation. Eur J Immunol 2001, 31:2669–2679
36. Wang S, Fan Y, Han X, Yang J, Bilenki L, Yang X: IL-12-dependent vascular cell adhesion molecule-1 expression contributes to airway eosinophilic inflammation in a mouse model of asthma-like reaction. J Immunol 2001, 166:2741–2749
37. Oppmann B, Lesley R, Blom B, Timans JC, Xu Y, Hunte B, Vega F, Yu N, Wang J, Singh K, Zonin F, Vaisberg E, Churakova T, Liu M, Gorman D, Wagner J, Zurawski S, Liu Y, Abrams JS, Moore KW, Rennick D, de Waal-Malefyt R, Hannum C, Bazan JF, Kastelein RA: Novel p19 protein engages IL-12p40 to form a cytokine, IL-23, with biological activities similar as well as distinct from IL-12. Immunity 2000, 13:715–725
38. Camoglio L, Juffermans NP, Peppelenbosch M, te Velde AA, ten Kate FJ, van Deventer SJ, Kopf M: Contrasting roles of IL-12p40 and IL-12p35 in the development of hapten-induced colitis. Eur J Immunol 2002, 32:261–269
39. Belladonna ML, Renauld JC, Bianchi R, Vacca C, Fallarino F, Orabona C, Fioretti MC, Grohmann U, Puccetti P: IL-23 and IL-12 have overlapping, but distinct, effects on murine dendritic cells. J Immunol 2002, 168:5448–5454
40. Trinchieri G: Interleukin-12: a proinflammatory cytokine with immunoregulatory functions that bridge innate resistance and antigen-specific adaptive immunity. Annu Rev Immunol 1995, 13:251–276
41. MacDonald TT, Monteleone G: IL-12 and Th1 immune responses in human Peyer's patches. Trends Immunol 2001, 22:244–247
42. D'Andrea A, Rengaraju M, Valiante NM, Chehimi J, Kubin M, Aste M, Chan SH, Kobayashi M, Young D, Nickbarg E, Chizzonite R, Wolf SF, Trinchieri G: Production of natural killer cell stimulatory factor (interleukin 12) by peripheral blood mononuclear cells. J Exp Med 1992, 176:1387–1398
43. Wittmann M, Kienlin P, Mommert S, Kapp A, Werfel T: Suppression of IL-12 production by soluble CD40 ligand: evidence for involvement of the p44/42 mitogen-activated protein kinase pathway. J Immunol 2002, 168:3793–3800
44. Young LS, Eliopoulos AG, Gallagher NJ, Dawson CW: CD40 and epithelial cells: across the great divide. Immunol Today 1998, 19:502–506

Intestinal villous M cells: An antigen entry site in the mucosal epithelium

Myoung Ho Jang[a,b], Mi-Na Kweon[a,b,c,d], Koichi Iwatani[a], Masafumi Yamamoto[a,d,e], Kazutaka Terahara[d,f], Chihiro Sasakawa[f,g], Toshihiko Suzuki[g,h], Tomonori Nochi[d,f], Yoshifumi Yokota[i], Paul D. Rennert[j], Takachika Hiroi[a,d,f], Hiroshi Tamagawa[a], Hideki Iijima[a], Jun Kunisawa[a,d], Yoshikazu Yuki[d,f], and Hiroshi Kiyono[a,d,f,k,l]

[a]Department of Mucosal Immunology, Research Institute for Microbial Diseases, Osaka University, Osaka 565-0871, Japan; [c]Mucosal Immunology Section, International Vaccine Institute, Seoul 151-818, Korea; [e]Department of Oral Medicine, Nihon University, School of Dentistry at Matsudo, Chiba 271, Japan; [g]Division of Bacteriology, Institute of Medical Science, University of Tokyo, Tokyo 108-8639, Japan; [h]PRESTO (Precursory Research for Embryonic Science and Technology), Japan Science and Technology Corporation (JST), Kawaguchi, Saitama 332-0012, Japan; [i]First Department of Biochemistry, Fukui Medical University, Matsuoka, Fukui 910-1193, Japan; [j]Biogen Incorporated, Cambridge, MA 02142; [f]Core Research for Evolutional Science and Technology (CREST), Japan Science and Technology Corporation (JST), Kawaguchi, Saitama 332-0012, Japan; [k]Immunobiology Vaccine Center, University of Alabama at Birmingham, Birmingham, AL 35294; and [d]Division of Mucosal Immunology, Institute of Medical Science, University of Tokyo, Tokyo 108-8639, Japan

Communicated by Roy Curtiss, Washington University, St. Louis, MO, February 11, 2004 (received for review September 20, 2003)

M cells located in the follicle-associated epithelium of Peyer's patches (PP) are shown to be the principal sites for the sampling of gut luminal antigens. Thus, PP have long been considered the gatekeepers of the mucosal immune system. Here, we report a distinct gateway for the uptake of gut bacteria: clusters of non-follicle-associated epithelium-associated *Ulex europaeus* agglutinin (UEA)-1$^+$ cells, which we have designated intestinal villous M cells. Interestingly, villous M cells are developed in various PP [or gut-associated lymphoid tissue (GALT)]-null mice, such as *in utero* lymphotoxin β receptor (LTβR)-Ig-treated, lymphotoxin α (LTα)$^{-/-}$, tumor necrosis factor/LT$\alpha^{-/-}$, and inhibition of differentiation 2 (Id2)$^{-/-}$ mice. Intestinal villous M cells have been observed to take up GFP-expressing *Salmonella*, *Yersinia*, and *Escherichia coli*-expressing invasin, as well as gut bacterial antigen for subsequent induction of antigen-specific immune responses. Thus, the identified villous M cells could be an alternative and PP-independent gateway for the induction of antigen-specific immune responses by means of the mucosal compartment.

The huge intestinal surface area is physically protected by a layer of tightly joined epithelial cells, which prevent most enteric environmental antigens from penetrating the host (1). However, entry into the host is made possible by a special gateway, comprised of M cells, located over organized mucosal lymphoid follicles such as Peyer's patches (PP). The M cells, characterized by an irregular brush border and reduced glycocalyx, efficiently take up and transport a wide variety of macromolecules and microorganisms from the gut lumen to the inside of the PP (2–6), which contain all of the necessary lymphoid cells for the induction and regulation of antigen-specific IgA responses (7). However, the origin of M cells and the regulation of their development are not understood. A previous study (8) showed that i.v. injection of PP lymphocytes into severe combined immunodeficient mice resulted in formation of new lymphoid follicles and follicle-associated epithelium (FAE) with typical M cells. A similar phenomenon was seen by using *in vitro* studies in which coculture with B lymphocytes triggered the conversion of enterocyte cell lines into M cell-like cells (9). Further, B cells have recently been proposed to play a role in the organogenesis of the mucosal immune barrier (10). Two different B cell-null mice, lacking expression of either μ membrane exon or the J_H segment of Ig genes, showed drastic reduction of FAE size and M cell numbers (10). In contrast, a recent study (11) demonstrated that the absence of mature T and B cells does not prevent the formation of FAE and M cells, and signaling of lymphotoxin (LT) α/β from non-B and non-T cells plays a critical role in formation of M cells in FAE of PP.

The common mucosal immune system (CMIS), which connects the inductive (e.g., PP) and effector (e.g., lamina propria; LP) sites, has been shown to be a central pathway for the induction of antigen-specific IgA immune responses in the gastrointestinal tract (7). For example, oral administration of *Salmonella typhimurium* leads to the transport of the bacterial antigen from the lumen of the intestinal tract into the PP by means of M cells for the initial priming of antigen-specific CD4$^+$ T cells and IgA-committed B cells (12). These antigen-sensitized cells leave the PP and contribute to the subsequent induction of *Salmonella*-specific IgA response in the distant intestinal LP by means of CMIS. In addition to the well-characterized CMIS-dependent IgA induction pathway, recent evidence suggests the presence of an additional IgA induction pathway that is independently operated from the PP-originated CMIS (13–15). Interestingly, it also has been reported that induction of intestinal mucosal IgA against the commensal bacteria was independent from T cell help and organized lymphoid tissue (16). Further, our recent study (17) has demonstrated that antigen-specific IgA antibody responses can be induced in the absence of PP. These studies imply the existence of a PP-independent mucosal immune pathway for dietary antigen and bacteria uptake.

A recent study (18) has suggested that the invasion gene (SPI1)-deficient *S. typhimurium* can be disseminated from the intestinal epithelium to the systemic compartment in the absence of PP-associated M cells by means of the CD18-dependent pathway. Further, dendritic cells in the lamina propria of the small intestine expressing tight junction protein offer another possible antigen uptake site (19). Thus, intestinal DCs are capable of extending dendrites to the lumen side by opening the tight junction. However, the exact mechanism for inducing Ag-specific immune responses independently of PP requires further elucidation.

In this study, we have discovered intestinal villous M cells, which serve as an antigen gateway for the sampling of gut bacteria and subsequent induction of Ag-specific immune responses in a PP-independent manner. These lines of study are crucial for understanding the mechanisms of antigen uptake from the gut lumen, and for the rational design of effective mucosal vaccines and optimal drug delivery across the gut.

Experimental Procedures

Mice. BALB/c and C57BL/6 mice were purchased from CLEA Japan (Tokyo). LTβR-Ig fusion protein-treated and tumor necrosis factor (TNF) and LTα double knockout (TNF/LT$\alpha^{-/-}$; 129 × C57BL/6) mice were generated as described (20, 21). LT$\alpha^{-/-}$ mice (C57BL/6) were obtained from The Jackson Laboratory. Inhibi-

Abbreviations: PP, Peyer's patches; FAE, follicle-associated epithelium; LT, lymphotoxin; TNF, tumor necrosis factor; WGA, wheat germ agglutinin; UEA, *Ulex europaeus* agglutinin; TRITC, tetramethylrhodamine B isothiocyanate; IEC, intestinal epithelial cell; ILF, isolated lymphoid follicle; GALT, gut-associated lymphoid tissue; Id2, inhibition of differentiation 2.

[b]M.H.J. and M.-N.K. contributed equally to this work.

[l]To whom correspondence should be addressed at the d address. E-mail: kiyono@ims.u-tokyo.ac.jp.

www.pnas.org/cgi/doi/10.1073/pnas.0400969101

tion of differentiation 2 $(Id2)^{-/-}$ mice (129/Sv) were generated as described (22).

M Cell Staining. A standard lectin staining procedure was used for the detection of murine M cells (23). Mucus-free small intestine of naive BALB/c or C57BL/6 mice, with or without PP, was fixed in 4% paraformaldehyde for 1 h, washed, and then blocked with 10% FBS in PBS containing 0.1% glycine. A lectin-labeling experiment was performed with *Ulex europaeus* agglutinin (UEA) conjugated with tetramethylrhodamine B isothiocyanate (TRITC) (UEA-1-TRITC, Vector Laboratories) and wheat germ agglutinin (WGA) conjugated with FITC (WGA-FITC) at a concentration of 20 μg/ml for 2 hr. After being rinsed in PBS, samples were stored in a Tris-buffered solution containing 30% glycerol and 0.1% NaN_3. The specimens were examined in a Bio-Rad MRC-600 confocal imaging system (Bio-Rad). Alkaline phosphatase activity and alcian blue staining were assessed on whole fixed small intestine as described (11). In addition, scanning and transmission electron microscopy analyses were performed for the characterization of M cells (see *Supporting Experimental Procedures*, which is published as supporting information on the PNAS web site).

Antigen Uptake *in Situ*. *S. typhimurium* PhoPc strain transformed with the pKKGFP plasmid was kindly provided by F. Niedergang (24, 25). Further, GFP-expressing *Yersinia pseudotuberculosis*, *Escherichia coli*-invasin, and *E. coli* were prepared by the method described (26, 27). Mice were anesthetized by i.p. injection of 2 mg of ketamine (Sigma) per mouse. Segments ≈10 cm long of the small intestine of $TNF/LT\alpha^{-/-}$ mice and wild-type mice were ligated at both ends with surgical thread. GFP-expressing bacteria (5×10^8) were suspended in 1.0 ml and inoculated into the loop and incubated *in situ*. Ten minutes later, PP and the intestinal segments (without PP) were removed and extensively washed with cold PBS and RPMI medium 1640 including gentamycin (100 μg/ml). Intestinal epithelial cells (IECs) were isolated from PP and the intestinal segments as described (28), then fixed in 4% paraformaldehyde, washed with 10% FBS in PBS, and labeled with UEA-1-TRITC. The percentage of double-positive IECs was analyzed on a FACSCalibur flow cytometer (Becton Dickinson). In selected mice, whole-mounted small intestinal segments were processed for confocal microscopy as described above. To remove weakly adhered and/or extracellular bacteria, vigorous washing with cold PBS and RPMI medium 1640 containing gentamycin were adopted during the process of isolation of villous epithelium including M cells and epithelial cells after infection with bacteria. Gentamycin was selected as the antibiotic due to its lethal effects on *Salmonella* (29). Therefore, our present data include only *Salmonella* that had strongly adhered and was intracellular but not *Salmonella* that was weakly adhered and extracellular.

Immunization. The recombinant *S. typhimurium* BRD 847 strain used in the immunization study is a double *aroA aroD* mutant that expresses the nontoxic, immunogenic 50-kDa ToxC fragment of tetanus toxin from plasmid pTET*nir*15 under the control of the anaerobically inducible *nirB* promoter (r*Salmonella*-ToxC) (30). For the control, r*Salmonella* that are not expressing ToxC were adopted. Recombinant *Salmonella* organisms were resuspended in PBS to a concentration of 2.5×10^{10} bacteria per ml. Bacterial suspensions were orally administered by gavage (0.2 ml per mouse). Ab titers in serum were determined by ELISA, as described elsewhere (17).

Data Analysis. Data were expressed as mean ± SD and evaluated by the Mann–Whitney *U* test. *P* values of <0.05 were assumed to be statistically significant.

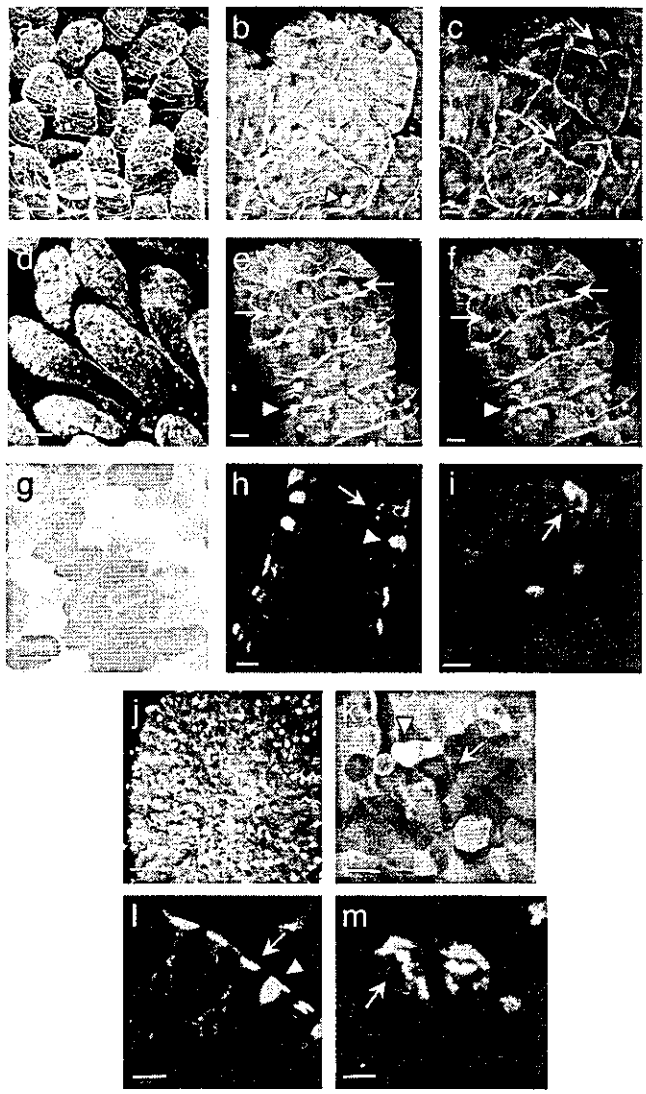

Fig. 1. Confocal view of UEA-1$^+$ cells in villous epithelium (*a–i*) and FAE of PP (*j–m*) isolated from naive BALB/c mice. M cell- and columnar epithelial cell-specific UEA-1-TRITC and WGA-FITC, respectively, were applied to the whole-mount preparation of the small intestine (*a–f*, *j*, and *k*). M cells were stained by UEA-1 (red, arrow), enterocytes by WGA (green), and goblet cells by UEA-1 and WGA (yellow, arrowhead). Villous M cells were found as two different distribution forms, dense (*a* and *b*) and diffuse (*d* and *e*) types. In contrast to the epithelial and goblet cells, M cells in the villous epithelium were completely negative to the WGA staining (*c* and *f*). Frozen sections were prepared and stained with UEA-1-TRITC alone (*h* and *l*) or with UEA-1-TRITC and B220 mAb-FITC (*i* and *m*) and the M cells were shown to have a pocket membrane and pocket lymphocytes (arrow) whereas the goblet cells do not (arrowhead). M cells were doubly negative cells for alkaline phosphatase activity demonstrated by red/pink color substrate, and alcian blue staining (white; *g*). The scale bar for *a*, *d*, and *j* is 50 μm; for *b*, *c*, *e*, *f*, *h*, and *l* is 20 μm; and for *g*, *i*, *k*, and *m* is 10 μm.

Results

Identification of Clusters of UEA-1$^+$ Cells in the Intestinal Villous Epithelium. M cells have been thought to be associated with, and to develop only in, the dome epithelium (or FAE) of mucosa-associated lymphoid tissues, e.g., PP. However, using confocal image analysis of whole-mount murine intestine stained with TRITC-conjugated UEA-1 and FITC-labeled WGA, we have found UEA-1$^+$WGA$^-$ cells not only in the FAE region of PP (Fig. 1 *j–l*), but also in the villous epithelium (Fig. 1 *a–i*). UEA-1, which possesses specificity for carbohydrate structures containing α(1–2)-fucose, selectively binds to the entire plasma membrane of PP M

cells but not to WGA$^+$ columnar epithelial cells (23). To further confirm the specificity of UEA-1 staining, we have performed a blocking experiment using 50 mM soluble fucose. Preincubation of the UEA-1 with soluble fucose for 1 hr clearly blocked UEA-1 staining in fluorescence-activated cell sorter (FACS, Becton Dickinson) and immunohistochemistry analyses further indicating the specificity of the UEA-1 staining method (data not shown). Interestingly, two forms of villous UEA-1$^+$WGA$^-$ cells, i.e., dense and diffuse, may be distinguished on the basis of the density of UEA-1$^+$WGA$^-$ cells (Fig. 1 *a* and *b* vs. *d* and *e*).

Our study revealed that these newly identified villous UEA-1$^+$WGA$^-$ cells share features with PP M cells but differ from goblet and columnar epithelial cells. Analysis of frozen sections of intestinal villi stained with TRITC-UEA-1 reveals that the villous UEA-1$^+$ cells possess the characteristic feature of M cells in PP FAE, i.e., a unique subdomain of the basolateral membrane, also known as the pocket membrane (Fig. 1*h*). The pocket lymphocytes were further confirmed by the staining with TRITC-UEA-1 and FITC-B220 mAb in villous UEA-1$^+$ cells (Fig. 1*i*) as well as in PP M cells (Fig. 1*m*).

Although they possess some affinity for UEA-1, goblet cells, unlike M cells, are capable as well of binding to WGA, making them doubly positive cells (UEA$^+$ WGA$^+$; Fig. 1 *b*, *e*, and *k*). In contrast to the epithelial and goblet cells, UEA-1$^+$ cells in the villous epithelium were completely negative for WGA staining (Fig. 1 *c* and *f*). Further, goblet cells are morphologically distinguished from M cells in that they do not possess the characteristic pocket membrane (Fig. 1 *h* and *i*). Intestinal columnar epithelial cells have high alkaline phosphatase (ALP) activity demonstrating with red or pink color, as do goblet cells stained with alcian blue, but M cells have neither of these features (11). Like PP M cells, villous UEA-1$^+$ cells in whole-mount intestinal samples were found to be negative for ALP activity and alcian blue staining (Fig. 1*g*). Thus, the UEA-1$^+$ cells, shown by our study to be analogous to PP M cells, have been designated villous M cells.

Development of Clusters of Villous UEA-1$^+$ M Cells in the Various PP-Null Mice. To further support this view, we examined whether villous M cells can develop in PP [or gut-associated lymphoid tissue (GALT)]-deficient mice, such as *in utero* LTβR-Ig-treated (21), LTα$^{-/-}$ (31), TNF/LTα$^{-/-}$ (20), and Id2$^{-/-}$ mice (22). We found M cells with the characteristic UEA-1$^+$ WGA$^-$ staining in the tip regions of intestinal villi of all PP-deficient mice (Fig. 2), thus documenting the presence of an FAE-independent M cell developmental pathway. This view was further supported by the presence of M cells in TNF/LTα$^{-/-}$ mice lacking newly described isolated lymphoid follicle (ILF) in addition to PP (data not shown). To define the distribution and number of villous M cell population in wild-type mice and GALT-null mice, we determined the frequency of the dense type of villous M cells in whole small intestine using the confocal imaging system. Approximately 40–50 dense-type villous M cell clusters were found per whole small intestine of wild-type mice. Similarly, ≈50–60 villous M cell clusters were found in the whole small intestine of TNF/LTα$^{-/-}$ mice, one of the representative GALT-null mice. The finding of similar numbers of villous M cells in the GALT-null and wild-type mice could suggest that the development of villous M cells is completely independent of GALT and FAE.

Attachment and Internalization of Bacteria by Villous M Cells. A further experiment was performed to gauge the ability of villous M cells to take up pathogenic microorganisms. Ligated small intestinal loops from wild-type mice were inoculated with r*Salmonella typhimurium* expressing green fluorescence (r*Salmonella*-GFP), *Yersinia pseudotuberculosis* (*Yersinia*-GFP), *E. coli*-expressing *Yersinia* invasin (*E. coli*-invasin-GFP), and wild-type *E. coli*-GFP. After a 10-min incubation with each bacteria *in situ*, sequential immunohistologic analyses of ligated small intestinal loops directly demonstrated the

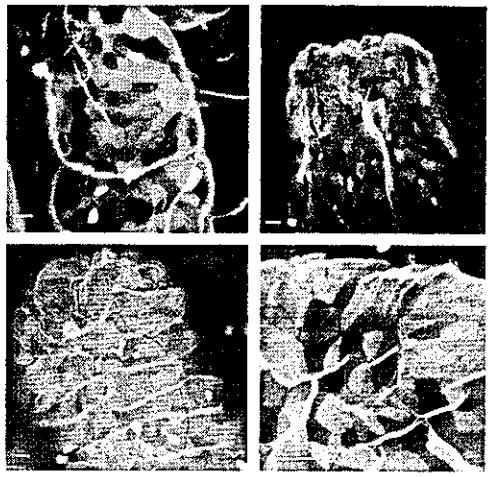

Fig. 2. The presence of villous M cells in PP-null mice, such as *in utero* LTβR-Ig-treated C57BL/6 mice (*Upper Left*), LTα$^{-/-}$ mice of C57BL/6 background (*Upper Right*), TNF/LTα$^{-/-}$ mice of 129 × C57BL/6 background (*Lower Left*), and Id2$^{-/-}$ mice of 129×Sv background (*Lower Right*). The scale bar for all pictures is 10 μm. The whole-mount preparations of small intestine were stained with FITC-WGA and TRITC-UEA-1.

presence of r*Salmonella*-GFP in UEA-1$^+$ cells in the villous epithelium of wild-type mice (Fig. 3 *Aa* and *Ab*) and TNF/LTα$^{-/-}$ mice (Fig. 3 *Ae* and *Af*). In addition, *Yersinia*-GFP was also specifically adhered to villous UEA-1$^+$ cells of wild-type mice (Fig. 3 *Ac* and *Ad*) and TNF/LTα$^{-/-}$ mice (Fig. 3 *Ag* and *Ah*). Immunohistologic analyses using frozen sections showed that r*Salmonella*-GFP was located in the apical membrane regions of villous UEA-1$^+$ cells (Fig. 3 *Ai* and *Aj*). To show the ability of villous UEA-1$^+$ cells to take up bacteria, we performed an ileal loop infection experiment using *rSalmonella*-GFP and analyzed the localization of bacteria with sequential confocal microscopy (Fig. 3*B*). Sequential Z plans of whole mount staining revealed the localization of *rSalmonella*-GFP in the intracellular region (Fig. 3 *B a–c*). In addition, *rSalmonella*-GFP was found in the intracellular region of villous UEA-1$^+$ cells prepared by cytospin (Fig. 3*Bd*).

Intestinal epithelial cells were further isolated from villous epithelium and PP after ileal loop injection of the microorganism expressing GFP, and then counterstained with TRITC-UEA-1 for flow cytometry analysis. We found a higher frequency of r*Salmonella*-GFP-, *Yersinia*-GFP-, or *E. coli*-invasin-GFP-containing cells in the fraction of UEA-1$^+$ cells than in the UEA-1$^-$ cells isolated from villous epithelium (Fig. 3*C*), and similar patterns were noted for the UEA-1$^+$ and UEA-1$^-$ cells isolated from the dome region of PP. In addition, high numbers of r*Salmonella*-GFP-, *Yersinia*-GFP-, or *E. coli*-invasin-GFP-containing cells were also recovered from UEA-1$^+$ but not UEA-1$^-$ cells isolated from the villous epithelium of TNF/LTα$^{-/-}$ mice lacking GALT (Fig. 3*C*). Taken together, these results indicate that villous M cells have the ability to take up several different bacteria from the lumen known to be taken up by FAE-M cells.

Scanning and Transmission Electron Microscope Analysis of Villous M Cells. Scanning electron microscopy (SEM) of the villous M cells revealed a hallmark feature of M cells, i.e., a depressed surface with short and irregular microvilli (Fig. 4 *a*, *b*, and *c*), seen also in the M cells of PP (Fig. 4 *d* and *e*). Transmission electron microscopy analysis also showed the binding of gold particle-conjugated UEA-1$^+$ cells in the villous M cells (Fig. 4 *f* and *g*). Further, the presence of infiltrating mononuclear cells was also seen in the pocket of villous M cells (Fig. 4*h*). The SEM also demonstrated the binding of bacteria to the membrane of villous M cells in the small intestine of FAE-null TNF/LTα$^{-/-}$ mice after intestinal exposure

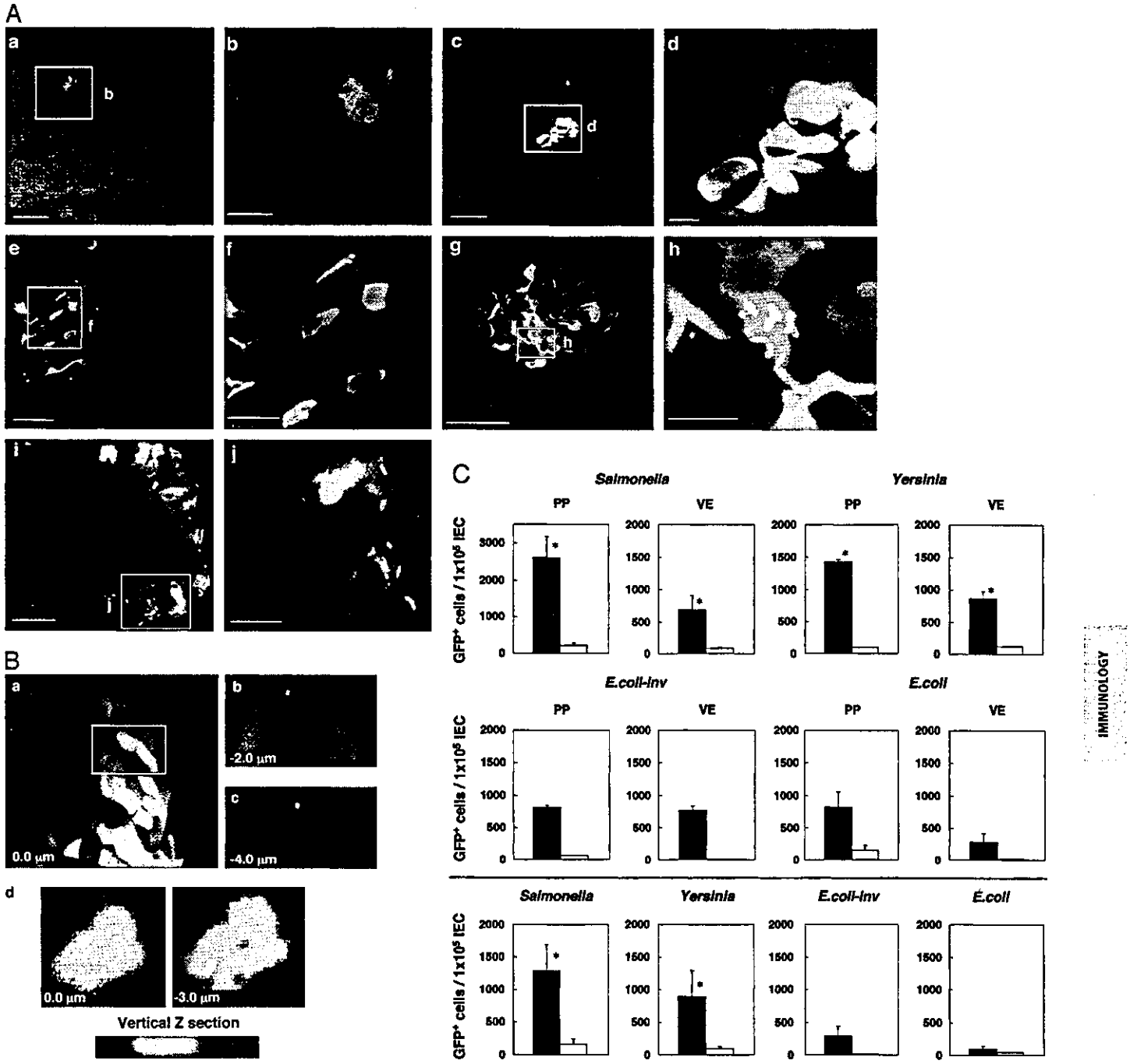

Fig. 3. (*A*) Immunohistochemistry for antigen uptake by UEA-1$^+$ villous M cells. Each panel shows histological features for sampling of GFP-expressing *Salmonella* (*a*, *b* and *e*, *f*) and *Yersinia* (*c*, *d* and *g*, *h*) by UEA$^+$ cells in the small intestine of wild-type (*a–d*) and PP-null TNF/LT$\alpha^{-/-}$ mice (*e–j*). Whole mount (*a–d* and *e–h*) and frozen sections of small intestine after exposure of GFP-expressing *Salmonella* were prepared and stained with UEA-1-TRITC (*i* and *j*). The scale bars are as follows: for *a*, *c*, and *g*, 50 μm; for *b*, *e*, and *i*, 20 μm; and for *d*, *f*, *h*, and *j*, 10 μm. (*B*) Localization of GFP-expressing *Salmonella* in the intracellular region of UEA-1$^+$ villous M cells. An ileal loop infection experiment using *rSalmonella*-GFP was performed for 30 min, and whole-mount tissues and UEA-1$^+$ IEC cells were analyzed by sequential confocal planar microscopy. Sequential Z plans of whole-mount staining revealed the localization of *rSalmonella*-GFP in the intracellular region of villous UEA-1$^+$ cells (*a*, *b*, and *c*). Further, the cytospin analysis revealed that *rSalmonella*-GFP also existed in the intracellular region of villous UEA-1$^+$ cells (*d*). (*C*) Antigen uptake by UEA-1$^+$ villous M cells. Cells (5×10^8) of GFP-expressing *S. typhimurium* PhoPc (*Salmonella*), *Y. pseudotuberculosis* (*Yersinia*), *E. coli*-invasin (*E. coli*-Inv), and *E.-coli* were administered into a 10-cm loop of the small intestine of naive wild-type mice (*Top* and *Middle*) or TNF/LT$\alpha^{-/-}$ mice (*Bottom*). After 10 min of incubation *in situ*, IECs were isolated from PP and villous epithelium. After being fixed with 4% paraformaldehyde, IECs were stained by UEA-1-TRITC, and uptake efficiency was analyzed by fluorescence-activated cell sorter (FACS). Data demonstrate the frequency of GFP$^+$ cells in the UEA$^+$ (filled bar) and UEA$^-$ (open bar) cells isolated from PP and villous epithelium (VE). The results represent the mean values ± SD from three separate experiments (three mice per group). *, $P < 0.05$ vs. the UEA$^-$ IEC group.

of *Salmonella* (Fig. 4 *i–l*). These findings provide supportive evidence that the newly identified villous M cell formed an alternative gateway for antigen sampling and/or entry from the lumen of intestinal villous epithelium. These findings provide evidence that M cells are developed and localized in the villous epithelium as well as in the FAE of PP.

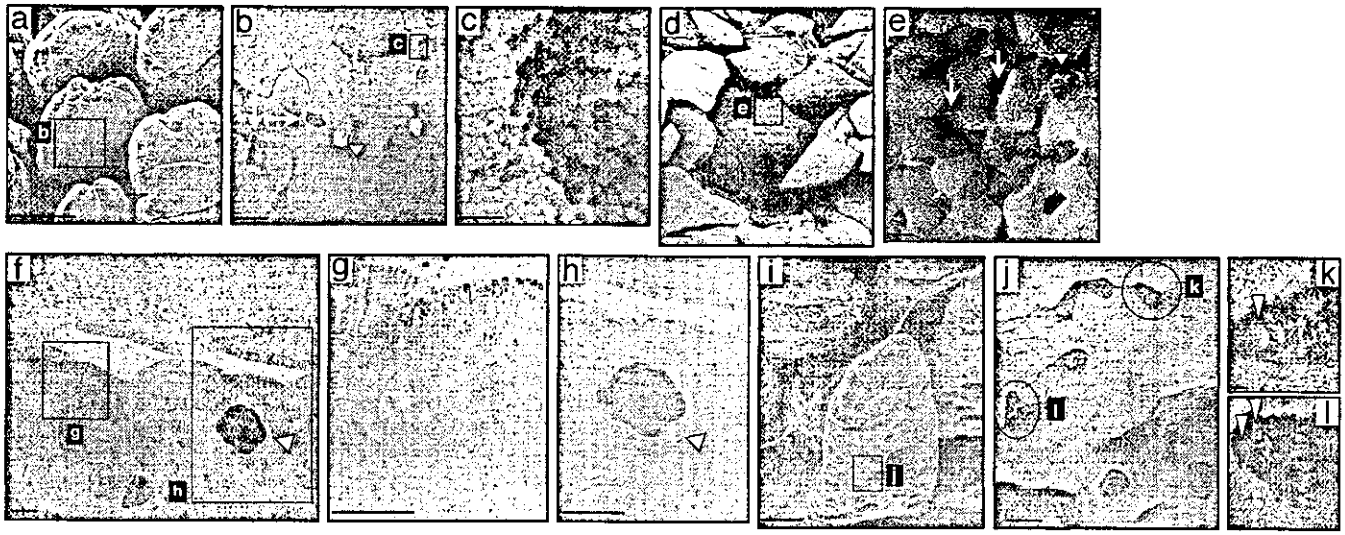

Fig. 4. Scanning and transmission electron microscopy of M cells in villous epithelium and FAE. Scanning electronic microscopy demonstrates that the M cells (arrow) in villous epithelium (*a–c*) and PP (*d* and *e*) are distinguished from enterocytes and goblet cells (arrowhead) by their relatively depressed and dark brush border. A transmission electron microscopy view of villous M cells shows short stub-like microvilli (*f*, *g*, and *h*) and the presence of infiltrating mononuclear cells in the pocket of villous M-cells (*h*; arrowhead). (*i–l*) The presence of villous M cells and the uptake of bacteria in the villous epithelium (arrowhead) after intestinal exposure of *Salmonella* (see Fig. 3 legend) in PP-deficient TNF/LT$\alpha^{-/-}$ mice. The scale bars are as follows: for *a*, *d*, and *i*, 50 μm; for *b*, *e*, *f*, and *j*, 5 μm; for *g* and *h*, 1.0 μm; and for *c*, *k*, and *l*, 0.5 μm.

Induction of Ag-Specific Immune Responses in PP-Deficient Mice. Our next experiments sought to examine whether antigen-specific antibody responses could be induced in GALT-deficient mice by means of the villous M cells. When GALT-null mice with TNF/LTα gene deficiency and wild-type mice were immunized orally with r*S. typhimurium* BRD 847 expressing a 50-kDa ToxC fragment of tetanus toxin (r*Salmonella*-ToxC), titers of tetanus toxoid (TT)-specific serum IgG antibodies were as high in the serum of the TNF/LT$\alpha^{-/-}$ mice as in orally immunized wild-type mice (Fig. 5). Expectedly, levels of TT-specific serum IgG antibody titers were not detectable when wild-type and TNF/LT$\alpha^{-/-}$ mice were orally immunized with r*Salmonella* not expressing ToxC (under the 5 of reciprocal $\log_2$ titer in Fig. 5). These findings suggest that the villous M cells are an important antigen-sampling site for the induction of antigen-specific immune responses to gastrointestinal environmental antigens.

Discussion

Because there is currently no reliable identified gene and corresponding antigen marker that positively identified M cells, the phenotype of M cells is defined by a combination of criteria including (3, 4) (*i*) the presence of the fucose epitope defined by the lectin UEA on M cell membrane, (*ii*) short and irregular microvilli, (*iii*) endocytic activity and ability to take up bacteria as well as macromolecules, and (*iv*) an intraepithelial pocket that allows a cluster of lymphocytes to be located in the epithelium. Based on our present results, villous M cells share all of the identifying features necessary to identify M cells found in the FAE of PP. Although M cell development has been thought to depend on FAE in organized mucosal lymphoid tissues, our results provide evidence that it can occur in the villous epithelium even in the absence of FAE. Further, these villous M cells are a gateway for entry or sampling of bacteria (e.g., *Salmonella*-, *Yersinia*-, and *E.-coli*-expressing invasin) for the subsequent induction of antigen-specific immune responses.

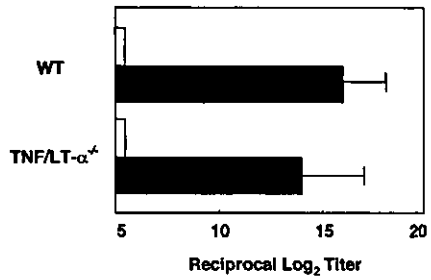

Fig. 5. Induction of Ag-specific immune responses in PP-deficient mice. Shown are PP-deficient (TNF/LT$\alpha^{-/-}$) and wild-type mice, which were orally immunized with r*Salmonella*-ToxC (filled bar) or r*Salmonella* alone (open bar). Serum samples were obtained 21 days after oral immunization for the assessment of tetanus toxoid (TT)-specific antibody responses by ELISA. The results represent the mean values ± SD from three separate experiments (three mice per group). There is no statistically significant difference between TNF/LT$\alpha^{-/-}$ and wild-type mice analyzed by unpaired Mann–Whitney *U* test.

M cells have been identified and documented only in the FAE-associated epithelium and occasionally on villi immediately adjacent to the lymphoid follicle (4, 32). A previous study (32) indicated that isolated M cells were found in the villous epithelium near the PP of the rabbit small intestine. In addition, clusters of UEA-1$^+$ cells in the small intestinal villi of conventional mice have been reported (33). These two studies suggested the existence of UEA-1$^+$ cells in the small intestinal villi of rabbit and mouse but did not address their identity or biological function. In this regard, our present study provides evidence of the existence of M cells in the villous epithelium away from PP of not only wild-type mice but also GALT-null mice. Further, our present results directly demonstrate the functional aspect of the villous M cells as a gateway for bacteria. Thus, we have substantially advanced the case that villous M cells are distinct from FAE-associated M cells in PP and have further shown that these villous M cells are a biologically important component of the mucosal immune system.

As discussed above, M cells reportedly are occasionally found in the villous epithelium adjacent to rabbit PP (32); however, we stress that villous M cells are located quite a distance from PP. Although the exact source of M cells has yet to be pinpointed, it is widely held that their development and localization are always associated with the organized lymphoid tissue of mucosal surfaces (e.g., PP). Our findings presented here, however, challenge this common assumption by providing evidence that M cells can be developed in villous epithelium in the absence of the FAE thought to be necessary to

their development in the organized mucosal lymphoid tissue. The diverse cellular phenotypes in the intestinal epithelium arise from crypt stem cells whose differentiation pathways can be modified by endogenous and exogenous influences (33–37). A previous study (34) demonstrated that *Streptococcus pneumoniae*-treated FAE tissues showed a marked increase in both IEL and epithelial cells with morphological and functional features of M cells. Further, enterocytes located in the peripheral of the FAE were converted into operational M cells as early as one hour after *in vivo* exposure to *S. pneumoniae* (32). Interestingly, expression of α1,2-linked fucosylated glyconjugates in the ileal epithelium was induced by the flora (33). Further, our unpublished data indicate that significantly increased numbers of UEA-1$^+$ cells in the villous epithelium of both wild-type and PP-null mice were detected after *in vivo* exposure to *S. typhimurium*. Therefore, it is possible that newly identified villous M cells can be developed from epithelial cells in response to foreign antigens and/or pathogens in the gut lumen. An interesting possibility would be that these UEA-1$^+$ crypt cells could be programmed to develop into the villous UEA-1$^+$ M cells after exposure to the exogenous microorganisms.

M cells in the FAE provide an entry site for pathogens, such as *S. typhimurium*, *Mycobacterium bovis*, *Shigella flexneri*, *Y. enterocolitica* and retroviruses (4, 38–40). It is well known that the invasion genes of the *Salmonella* pathogenicity island (SPI1) are necessary for the entry of *S. typhimurium* into FAE-M cells and epithelial cells (38, 41). However, SPI1-deficient *Salmonella* is transported from the gastrointestinal tract to the blood stream by CD18-expressing phagocytes, and CD18-deficient mice were shown to be resistant to orally administered *Salmonella* (18). Overall, it seems likely that several cell types, including M cells, epithelial cells, and CD18-expressing macrophages, are involved in permitting the penetration of *Salmonella*. On the other hand, previous studies have showed that *Y. enterocolitis* selectively and specifically invades the FAE of PP by means of M cells but not by means of other cells (42, 43). Interestingly, it has been suggested $\alpha_4\beta_1$ integrin is expressed on the apical membranes of M cells but not on villous or dome epithelial enterocytes, implying that this integrin may be exploited by *Yersinia* to attach to and invade the M cells (44). Further, invasin mediates uptake of *Y. pseudotuberculosis* into mammalian cells through binding with β1-chain integrins with high affinity (45, 46). In light of these complexities, the fact that villous M cells and FAE-associated M cells in PP sampled GFP-expressing *Salmonella*, *Yersinia*, and *E. coli*-invasin suggests that villous M cells likely possess a capacity of playing as professional bacteria translocating cells.

A recent study (13) has provided new evidence that IgA-specific B cell responses including isotype-switching can be induced in intestinal lamina propria without the influence of PP. In addition, our recent study showed that ILF in the small intestine are structurally and functionally similar to the PP and contain M cells on their FAE region (47). To eliminate the possible role of M cells associated with the ILF for antigen sampling, we used TNF/LT$\alpha^{-/-}$ mice, which lack both PP (17) and ILF (unpublished data). Interestingly, high numbers of GFP-expressing *Salmonella*, *Yersinia*, and *E. coli*-invasin were recovered from UEA-1$^+$ but not UEA-1$^-$ cells isolated from the villous epithelium of TNF/LT$\alpha^{-/-}$ mice although the total uptake of GFP$^+$ eukaryotic cells was less pronounced than in wild-type mice (Fig. 3*C*). Together with the data for the induction of antigen-specific antibody responses after oral immunization in these PP- and ILF-deficient mice (Fig. 5), our results provide a strong case that villous M cells are an alternative gateway of antigen entry for the mucosal immune system. On the other hand, a recent study (19) showed that antigen sampling occurs across the non-FAE by mucosal intraepithelial dendritic cells. Thus, it is still possible that antigen-specific immune responses seen in TNF/LT$\alpha^{-/-}$ mice could be initiated by means of these intraepithelial dendritic cells.

In summary, our observations indicate that typical M cells can develop without the influence of the FAE associated with mucosal lymphoid tissue such as PP and in fact are present in villous epithelium. Moreover, villous M cells may be an alternative gateway for the penetration of pathogenic microorganisms as well as an additional antigen-sampling site for the induction of antigen-specific immune responses by means of the mucosal tissues.

We thank Mr. Takashi Wada for helpful technical assistance with scanning electron microscopy. We thank Drs. William R. Brown and Kimberly McGhee for editing the manuscript and Drs. Ichiro Takahashi, Jean-Pierre Kraehenbuhl, and Satoshi Fukuyama for helpful discussions and suggestions. This work was supported by grants from Core Research for Evolutional Science and Technology (CREST) of the Japan Science and Technology Corporation (JST), the Ministry of Education, Science, Sports, and Culture, and the Ministry of Health and Welfare in Japan, as well as by SRC fund to IRC at the University of Ulsan from Korea Science and Engineering Foundation (KOSEF) and the Korean Ministry of Science and Technology.

1. Madara, J. L. (1998) *Annu. Rev. Physiol.* **60**, 143–159.
2. Frey, A., Giannasca, K. T., Weltzin, R., Giannasca, P. J., Reggio, H., Lencer, W. I. & Neutra, M. R. (1996) *J. Exp. Med.* **184**, 1045–1059.
3. Kraehenbuhl, J. P. & Neutra, M. R. (2000) *Annu. Rev. Cell Dev. Biol.* **16**, 301–332.
4. Neutra, M. R., Frey, A. & Kraehenbuhl, J. P. (1996) *Cell* **86**, 345–348.
5. Neutra, M. R., Mantis, N. J., Frey, A. & Giannasca, P. J. (1999) *Semin. Immunol.* **11**, 171–181.
6. Owen, R. L. (1977) *Gastroenterology* **72**, 440–451.
7. Mestecky, J., Blumberg, R. S., Kiyono, H. & McGhee, J. R. (2003) in *Fundamental Immunology*, ed. Paul, W. E. (Lippincott Williams & Wilkins), 5th Ed., p. 965.
8. Savidge, T. C. & Smith, M. W. (1995) *Adv. Exp. Med. Biol.*, **371**, 239–241.
9. Kemeis, S., Bogdanova, A., Kraehenbuhl, J. P. & Pringault, E. (1997) *Science* **277**, 949–952.
10. Golovkina, T. V., Shlomchik, M., Hannum, L. & Chervonsky, A. (1999) *Science* **286**, 1965–1968.
11. Debard, N., Sierro, F., Browning, J. & Kraehenbuhl, J. P. (2001) *Gastroenterology* **120**, 1173–1182.
12. VanCott, J. L., Kobayashi, T., Yamamoto, M., Pillai, S., McGhee, J. R. & Kiyono, H. (1996) *Vaccine* **14**, 392–398.
13. Fagarasan, S., Kinoshita, K., Muramatsu, M., Ikuta, K. & Honjo, T. (2001) *Nature* **413**, 639–643.
14. Hiroi, T., Yanagita, M., Iijima, H., Iwatani, K., Yoshida, T., Takatsu, K. & Kiyono, H. (1999) *J. Immunol.* **162**, 821–828.
15. Hiroi, T., Yanagita, M., Ohta, N., Sakaue, G. & Kiyono, H. (2000) *J. Immunol.* **165**, 4329–4337.
16. Macpherson, A. J., Gatto, D., Sainsbury, E., Harriman, G. R., Hengartner, H. & Zinkernagel, R. M. (2000) *Science* **288**, 2222–2226.
17. Yamamoto, M., Rennert, P., McGhee, J. R., Kweon, M. N., Yamamoto, S., Dohi, T., Otake, S., Bluethmann, H., Fujihashi, K. & Kiyono, H. (2000) *J. Immunol.* **164**, 5184–5191.
18. Vazquez-Torres, A., Jones-Carson, J., Baumler, A. J., Falkow, S., Valdivia, R., Brown, W., Le, M., Berggren, R., Parks, W. T. & Fang, F. C. (1999) *Nature* **401**, 804–808.
19. Resigno, M., Urbano, M., Valzasina, B., Francolini, M., Rotta, G., Bonasio, R., Granucci, F., Kraehenbuhl, J. P. & Ricciardi-Castagnoli, P. (2001) *Nat. Immunol.* **2**, 361–367.
20. Eugster, H. P., Muller, M., Karrer, U., Car, B. D., Schnyder, B., Eng, V. M., Woerly, G., Le Hir, M., di Padova, F., Aguet, M., Zinkernagel, R., Bluethmann, H. & Ryffel, B. (1996) *Int. Immunol.* **8**, 23–36.
21. Rennert, P. D., Browning, J. L., Mebius, R., Mackay, F. & Hochman, P. S. (1996) *J. Exp. Med.* **184**, 1999–2006.
22. Yokota, Y., Mansouri, A., Mori, S., Sugawara, S., Adachi, S., Nishikawa, S. & Gruss, P. (1999) *Nature* **397**, 702–706.
23. Gebert, A., Fassbender, S., Werner, K. & Weissferdt, A. (1999) *Am. J. Pathol.* **154**, 1573–1582.
24. Hopkins, S. A., Niedergang, F., Corthesy-Theulaz, I. E. & Kraehenbuhl, J. P. (2000) *Cell. Microbiol.* **2**, 59–68.
25. Niedergang, F., Sirard, J. C., Blanc, C. T. & Kraehenbuhl, J. P. (2000) *Proc. Natl. Acad. Sci. USA* **97**, 14650–14655.
26. Bolin, I. & Wolf-Watz, H. (1984) *Infect. Immun.* **43**, 72–78.
27. Rosqvist, R., Skurnik, M. & Wolf-Watz, H. (1988) *Nature* **334**, 522–524.
28. Yamamoto, M., Fujihashi, K., Kawabata, K., McGhee, J. R. & Kiyono, H. (1998) *J. Immunol.* **160**, 2188–2196.
29. Elsinghorst, E. A. (1994) *Methods Enzymol.* **236**, 405–420.
30. Chatfield, S. N., Charles, I. G., Makoff, A. J., Oxer, M. D., Dougan, G., Pickard, D., Slater, D. & Fairweather, N. F. (1992) *Biotechnology (N.Y.)* **10**, 888–892.
31. De Togni, P., Goellner, J., Ruddle, N. H., Streeter, P. R., Fick, A., Mariathasan, S., Smith, S. C., Carlson, R., Shornick, L. P., Strauss-Schoenberger, J., *et al.* (1994) *Science* **264**, 703–707.
32. Borghesi, C., Taussig, M. J. & Nicoletti, C. (1999) *Lab. Invest.* **79**, 1393–1401.
33. Bry, L., Falk, P. G., Midtvedt, T. & Gordon, J. I. (1996) *Science* **273**, 1380–1383.
34. Borghesi, C., Regoli, M., Bertelli, E. & Nicoletti, C. (1996) *J. Pathol.* **180**, 326–332.
35. Meynell, H. M., Thomas, N. W., James, P. S., Holland, J., Taussig, M. J. & Nicoletti, C. (1999) *FASEB J.* **13**, 611–619.
36. Sierro, F., Pringault, E., Assman, P. S., Kraehenbuhl, J. P. & Debard, N. (2000) *Gastroenterology* **119**, 734–743.
37. Slack, J. M. (2000) *Science* **287**, 1431–1433.
38. Jones, B. D., Ghori, N. & Falkow, S. (1994) *J. Exp. Med.* **180**, 15–23.
39. Wassef, J. S., Keren, D. F. & Mailloux, J. L. (1989) *Infect. Immun.* **57**, 858–863.
40. Wolf, J. L., Rubin, D. H., Finberg, R., Kauffman, R. S., Sharpe, A. H., Trier, J. S. & Fields, B. N. (1981) *Science* **212**, 471–472.
41. Galan, J. E. & Curtiss, R., 3rd (1989) *Proc. Natl. Acad. Sci. USA* **86**, 6383–6387.
42. Autenrieth, I. B. & Firsching, R. (1996) *J. Med. Microbiol.* **44**, 285–294.
43. Autenrieth, I. B., Vogel, U., Preger, S., Heymer, B. & Heesemann, J. (1993) *Infect. Immun.* **61**, 2585–2595.
44. Clark, M. A., Hirst, B. H. & Jepson, M. A. (1998) *Infect. Immun.* **66**, 1237–1243.
45. Isberg, R. R. & Leong, J. M. (1990) *Cell* **60**, 861–871.
46. Isberg, R. R., Voorhis, D. L. & Falkow, S. (1987) *Cell* **50**, 769–778.
47. Hamada, H., Hiroi, T., Nishiyama, Y., Takahashi, H., Masunaga, Y., Hachimura, S., Kaminogawa, S., Takahashi-Iwanaga, H., Iwanaga, T., Kiyono, H., *et al.* (2002) *J. Immunol.* **168**, 57–64.

Available online at www.sciencedirect.com

SCIENCE DIRECT

Clinical Immunology 113 (2004) 326–339

CLINICAL IMMUNOLOGY

www.elsevier.com/locate/yclim

Biological role of Ep-CAM in the physical interaction between epithelial cells and lymphocytes in intestinal epithelium

Tomonori Nochi[a,b,c], Yoshikazu Yuki[a,c], Kazutaka Terahara[a,c], Ayako Hino[a,c], Jun Kunisawa[a], Mi-Na Kweon[a,d], Takahiro Yamaguchi[b], Hiroshi Kiyono[a,c,*]

[a]*Division of Mucosal Immunology, Department of Microbiology and Immunology, The Institute of Medical Science, The University of Tokyo, Tokyo 108-8639, Japan*

[b]*Laboratory of Functional Morphology, Division of Life Science, Department of Animal Biology, The Graduate School of Agricultural Science, Tohoku University, 981-8555, Japan*

[c]*CREST, Japan Science and Technology, 332-0012, Japan*

[d]*Division of Mucosal Immunology, International Vaccine Institute, 151-600, South Korea*

Received 13 August 2004; accepted with revision 24 August 2004
Available online 29 September 2004

Abstract

The mucosal epithelium including intestinal epithelial cells (IECs) and intraepithelial lymphocytes (IELs) provide a first line of defense in the gastrointestinal tract. However, limited information is currently available concerning the nature of the physical interaction molecule that interconnects IECs and IELs. Among the several monoclonal antibodies (mAbs) generated by immunizing porcine IECs, mAb (5-15-1) was shown to strongly react with IELs in addition to IECs. MALDI-TOF-MS and tandem MS analysis suggested that the antigen belongs to a family of human homophilic epithelial cell adhesion molecule (Ep-CAM). The amino acid sequence of porcine Ep-CAM showed 82.8%, 78.1%, and 76.8% homology compared to human, mouse, and rat Ep-CAM. Moreover, 5-15-1 specifically reacted with transfectant of porcine Ep-CAM. These data suggest that the Ep-CAM may act as a physical homophilic interaction molecule between IELs and IECs at the mucosal epithelium for providing immunological barrier as a first line of defense against mucosal infection.

Keywords: Mucosa; Epithelial cell; Intraepithelial lymphocyte; Adhesion molecule; Cell surface molecule; Cell trafficking

Introduction

Intestinal epithelial cells (IECs) originate from and are maintained by a small number of pluripotent stem cells in crypts and have a life span of 2–4 days [1]. IECs have long been known to absorb nutrients into the circulation. More recently, IECs have also been found to act as an important immunological barrier against pathogens or nonself antigens and thus to comprise a major compartment of the mucosal immune system. They are equipped with mucus and antibacterial enzymes (e.g., lysozyme), which act as innate barriers, and secretory IgA (S-IgA) and T cell-mediated immunity, which serve as acquired barriers [2]. To preserve the integrity of the first line of defense against pathogens, IECs are welded together by a number of adhesion mechanisms. For example, tight junctions consisting of occludin [3] and the family of claudin [4,5] have been shown to play a central role in sealing the intracellular space between epithelial cells [6–8]. E-cadherin, another adhesion molecule expressed by epithelial cells, homophilically regulates Ca^{2+}-dependent interactions at the site of the tight junction [9]. The extracellular domain of E-cadherin is composed of five repeats and contain Ca^{2+} binding motifs [10]. Cadherin forms tight complexes with three cytoplasmic proteins, α-, β-, and γ-catenin, linked to the actin cytoskeleton [11]. This unique cell-to-cell adhesion system

* Corresponding author. Division of Mucosal Immunology, Department of Microbiology and Immunology, The Institute of Medical Science, The University of Tokyo, 4-6-1 Shirokanedai, Minato-ku, Tokyo 108-8639, Japan. Fax: +81 3 5449 5411.
E-mail address: kiyono@ims.u-tokyo.ac.jp (H. Kiyono).

1521-6616/$ - see front matter © 2004 Elsevier Inc. All rights reserved.
doi:10.1016/j.clim.2004.08.013

of IECs helps maintain a physiologically normal intestinal epithelium by serving as both a physical and immunological barrier against the invasion of undesirable foreign substances. On the other hand, under the condition of sever mucosal inflammation (e.g., inflammatory bowel diseases), the expression of these epithelial intercellular junction proteins was down-regulated by transmigrating neutrophils from intestinal lamina propria to lumen [12]. Thus, a group of these adhesion molecules associating with the formation of mucosal epithelium is directly influenced by the process of development of inflammation.

Most intraepithelial lymphocytes (IELs), which are present in large numbers in the intestinal epithelium, are $CD3^+$ T cells and are expressed by heterodimer chains of either αβ or γδ T cell receptors (TCR). In mice, IEL expression is almost evenly divided between αβ and γδ TCR [13]. Although their exact immunological functions remain unknown, these IELs have been shown to be involved in both the innate and acquired phases of mucosal immunity [14]. IELs bearing γδTCR (γδIELs) possess several features that distinguish them from αβIELs. For example, γδIELs exclusively express the CD8αα homodimer or doubly negative for CD4 and CD8 and are thought to be developed extrathymically [15]. In addition, γδIELs are absent in mice lacking a common cytokine receptor γ chain, which is a subunit of the receptor for IL-2, IL-4, IL-7, IL-9, and IL-15 [16]. The unique immunological and microbiological environment of the intestinal epithelium perhaps contributes to the creation of subsets of IEL-associated T cells distinct from the thymus-originated T cells located in the peripheral lymph nodes.

A number of recent findings suggest that a reciprocal dependency exists between IECs and IELs and that it is under the regulation of a group of intestinal epithelium-associated cytokines, including IL-7, IL-15, and SCF [17–19]. IECs are capable of producing IL-7 and IL-15, important cytokines for the stimulation and development of γδIELs expressing the corresponding receptor [20–22], while γδIELs have been shown to produce SCF, which stimulates the growth of IECs [19]. These results clearly indicate that an array of interactions between cytokines and their corresponding receptors play an important role in the formation and maintenance of the monolayer of the mucosal epithelium. Further, it has been suggested that IECs and IELs form mucosal intranet and provide a first line of defense at mucosal epithelium [2]. IEC-derived IL-15 has been shown to be a key regulatory molecule for the generation of IELs including γδT cells-mediated immunological barrier function [23]. On the other hand, overproduction of IL-15 at the mucosal epithelium resulted in the development of intestinal inflammation [24]. A similar aberrant condition was also triggered by the overproduction of IL-7 at mucosal epithelium [25]. These findings further emphasize the importance of mucosal intranet operated by IECs and IELs for the control of inflammation and infection. However, minimal information is currently available regarding the cellular and molecular mechanisms underlying the physical cell-to-cell interactions between IECs and IELs via the cell surface adhesion molecule. To address this gap in the data, we have sought in this study to elucidate the molecular basis for the physical cell-to-cell interactions between IECs and IELs by generating monoclonal antibodies (mAbs) to react with the cell surface of both IECs and IELs.

Materials and methods

Animal

Female Balb/c mice (6 weeks old) were purchased from CREA (Tokyo, Japan) and maintained in the experimental animal facility at the Institute of Medical Science, the University of Tokyo. The tissues of male and female three-way cross-bred pigs were purchased from Tokyo Shibaura Zouki (Tokyo, Japan). All of the tissues were obtained from 6-month-old pigs. In some cases, the tissues were kindly provided from Chugai Research Institute for Medical Science (Nagano, Japan).

Isolation of porcine IECs from the small intestine

IECs were physically and enzymatically isolated from porcine small intestines. First, the small intestines were washed with cold PBS and then torn into muscle layers. The tissues were then cut into small fragments of 1–2 cm and digested with 1 mg/ml collagenase (Wako, Osaka, Japan) and 1 mg/ml hyaluronidase (Sigma, Saint Louis, MO) in PBS at 37°C for 20 min. After digestion, tissue was washed again with cold PBS and then redigested with 1 mg/ml pancreatin (Sigma) in 25 mM HEPES buffer at 37°C for 15 min. Isolated cells were washed with cold PBS and then purified using a 45% Percoll gradient (Amasham Pharmacia Biotech, Uppsala, Sweden). Following centrifugation, the upper layer of cells was collected and stained first with mouse IgG1 anti-porcine CD45 mAb (K252.1E4, Serotec Ltd., Oxford, UK) diluted 1:10 at 4°C for 30 min and then by microbead-conjugated rat anti-mouse IgG1 (Miltenyi Biotec, Bergisch Gladbach, Germany) diluted 1:5 at 4°C for 15 min to further remove contaminated leukocytes. Finally, IECs were negatively selected by auto-MACS (Miltenyi Biotec). Immunostaining with anti-cytokeratin mAb (Sigma) showed that the resulting IEC preparation was highly purified (>95%) [26].

Generation of mouse monoclonal antibodies

Purified porcine IECs were used for intraperitoneal immunization of BALB/c mice (2.0×10^6 cells/mouse). After 1 week, the mice received a booster intravenous injection of porcine IECs (1.0×10^6 cells/mouse). Four days after the booster, the mice were sacrificed so that splenic mononuclear cells could be harvested. Splenocytes

were fused with Sp2/0-Ag14 myeloma cells (ATCC, CRL-1581) in the presence of 50% (w/v) polyethylene glycol 1500 (Roche, Mannheim, Germany). Supernatants from the resulting hybridomas were screened with isolated cells from the small intestine by flow cytometry analysis. The isotype of the porcine IEC-reactive hybridoma was determined using a mouse monoclonal antibody-isotyping kit (Amersham Pharmacia Biotech). The mAbs, produced in the ascitic fluids of BALB/c mice by priming with pristane (Wako), were purified using Protein G sepharose (Amersham Pharmacia Biotech). Purified mAbs were biotinylated with EZ-Link Sulfo-NHS-LC-biotin (PIERCE, Rockford, IL). Among 10 mAbs generated, one clone of mAb (5-15-1: mouse IgG2b) was selected for the present study due to its specific and strong reactivity with the porcine intestinal epithelium. An optimal concentration of mAb (5-15-1) was determined for the different assay system used in this study, and those doses are indicated for the respective protocol or figure legend.

Immunohistochemistry

The porcine tissues were fixed in 4% paraformaldehyde (Wako), incubated overnight at 4°C, and then washed with 8% and 16% (w/v) sucrose solutions before being incubated overnight again at 4°C. The tissues were then embedded in Tissue-Tek OCT compound (SAKURA Finetechnical Company, Ltd., Tokyo, Japan). Tissue sections (5 μm) were incubated with 1.5% (v/v) normal goat serum (Vector, Burlingame, CA) for 20 min at room temperature (RT). They were then incubated overnight at 4°C with 10 μg/ml purified mAb (5-15-1, mouse IgG2b) and/or anti-porcine CD45 mAb (mouse IgG1, Serotec, Ltd.) diluted 1:10 or an isotype control (mouse IgG1 and/or mouse IgG2b, BD PharMingen, San Jose, CA). For single staining, they were incubated with FITC-conjugated goat anti-mouse IgG (IMMUNOTECH, Marseille, France) diluted 1:200 for 1 h at RT, and for double staining with FITC-conjugated anti-mouse IgG2b (Santa Cruz Biotechnology, Santa Cruz, CA) diluted 1:100 and rhodamine-conjugated anti-mouse IgG1 (Santa Cruz Biotechnology) diluted 1:100. Finally, the sections were counterstained with 1 μg/ml propidium iodate (Sigma) or 200 ng/ml DAPI (Sigma) for 30 min at RT and analyzed using a confocal laser scanning microscope (TCS SP2, Leica, Wetzlar, Germany).

Immunoprecipitation and Western blot analysis

The lysate of several tissues were washed with cold PBS and lysed in lysis buffer [50 mM Tris–HCl (pH 7.5), 150 mM NaCl, 0.5% Triton X-100, and a protease inhibitor cocktail (Roche)]. After 1 h of incubation on ice followed by centrifugation, the lysate (5 mg/ml, 1 ml) was precleared with 40 μl protein G Sepharose (1:1 in PBS, Amersham Pharmacia Biotech) at 4°C for 1 h. After centrifugation, the lysate was incubated with mAb (5-15-1, 10 μg/ml) or an isotype control (mouse IgG2b, BD PharMingen) for 1 h at 4°C, before the addition of 40 μl Protein G Sepharose (1:1 in PBS) and incubation for 1 h at 4°C. Immune complexes were washed five times with cold PBS containing a protease inhibitor cocktail and eluted in Laemmli sample buffer with or without 2-ME. They were then subjected to an SDS-PAGE using a 12.5% polyacrylamide gel (Daiichi Pure Chemical, Tokyo, Japan) before being transferred to a polyvinylidene difluoride (PVDF) membrane (MILLIPORE, Billerica, MA) using a semidry transblot system (ATTO Instruments, Tokyo, Japan). The membranes were blocked in 1% BSA, 0.2% Tween-20/PBS overnight at 4°C, and incubated with biotinylated mAb (5-15-1, 10 μg/ml) at RT for 1 h and then with ABC-AP complex (Vector) at RT for 1 h. Finally, the reaction was detected with an Alkaline phosphatase-conjugated substrate kit (Bio-Rad, Hercules, CA). Carbohydrates were also stained with G.P. Sensor (HONEN, Yokohama, Japan) in accordance with the manufacturer's instructions.

Isolation of IELs, splenocytes, and PBMCs for flow cytometric analysis

Lymphocytes were isolated from small intestinal epithelium and spleen, as described previously with some modifications [26]. Briefly, in the case of IELs, the small intestinal epithelium was prepared and then stirred at 37°C in RPMI-1640 (Sigma) containing 1 mM EDTA for 20 min. Lymphocytes from the small intestinal epithelium and spleen were separated on a Percoll density gradient (Amersham Pharmacia Biotech). The cells layered between the 40% and 75% fractions were collected as IELs and splenocytes. PBMCs were separated on NycoPrep (AXIS-SHIELD PoC AS, Oslo, Norway) after blood was mixed with two volumes of PBS. IECs, IELs, splenocytes, and PBMCs were incubated with 1 μg/ml porcine IgG (Sigma) at 4°C for 20 min and then stained with 10 μg/ml purified mAb (5-15-1) or an isotype control (mouse IgG2b, BD PharMingen) at 4°C for 30 min, before being subjected to an FITC-conjugated anti-mouse IgG (IMMUNOTECH) and 10 μl/test VIAPROBE (BD Pharmingen) for 30 min at 4°C. Finally, the cells were analyzed by flow cytometry using FACSCalibur (Becton Dickinson, Franklin Lakes, NJ).

Purification and analysis of antigen by MALDI-TOF-MS and Tandem MS after triptic digestion

The antigen of mAb (5-15-1) was purified from the lysate of the small intestine by affinity chromatography using an Affi-Gel Hz Immunoaffinity Kit (Bio-Rad). Purified antigen was analyzed by SDS-PAGE with 12.5% polyacrylamide gel and stained by GelCode Blue Stain Reagent (PIERCE). The responding protein was digested with trypsin using a method previously described [27]. The resulting peptide samples were analyzed by time-of-flight mass spectrometry (Applied Biosystems, Foster, CA) after being spotted on a

MALDI plate and co-crystallized with α-cyano-4-hydroxycinnamic acid [27]. This plate was then loaded into the QSTAR Pulser *i* (Applied Biosystems) at Hitachi Science Systems (Ibaraki, Japan).

Cloning of porcine epithelial cell adhesion molecules (Ep-CAM)

The porcine Ep-CAM gene was amplified from the mRNA of the small intestine by RT-PCR with mix primers (Sense: 5′-CDKCYAARTGYTTGGYGATG-3′ Antisense: 5′-RMCACMACSACAATRACRGC-3′) prepared based on the sequence data from humans [28], mice [29], and rats [30]. The 5′ and 3′ regions were analyzed with a GeneRacer kit (Invitrogen, Carlsbad, CA) by oligocapping and 3′RACE methods with primers prepared by the sequence data obtained from the internal porcine Ep-CAM (5′ region: 5′-AGGTCCATCCTTTTGGAATG-3′, 5′-AGGTACCATTACACTGCTTG-3′, 3′ region: 5′-ATTACCAACTGGATCCCAAA-3′, 5′-ATGAATCCTTGTTCCA-TTCC-3′). The sequencing was performed using the ABI3700 at Hitachi Science Systems (Tokyo, Japan).

Transfection of cells

Full-length porcine Ep-CAM was amplified by RT-PCR with primers (sense:5′-ATTACTAATAGCTAGCATGGCGCCCCCCCAGGTCCT-3′, antisense: 5′-AGCACTGAATTCTTATGCATTGAGTTCCCTAT-3′, *Nhe*I, and *Eco*RI restriction enzyme site showed by underlining). It was then ligated into pIRES2-EGFP Vector (BD Biosciences Clontech, Palo Alto, CA) in front of the enhanced GFP (EGFP)-coding region at the *Nhe*I and *Eco*RI sites using the DNA Ligation Kit Ver.2 (Takara Biomedicals, Shiga, Japan) and sequenced. Because it contained the internal ribosome entry site (IRES), this plasmid (pIRES2-EGFP-pEp-CAM) was able to express both porcine Ep-CAM and EGFP. pIRES2-EGFP-pEp-CAM was transfected into COS-7 (ATCC, CRL-1651) in Opti-MEM (Invitrogen) by electrophoresis using Gene Pulser Xcell (Bio-Rad) [31]. After 48 h, the cells were stained first with 10 μg/ml mAb (5-15-1) or an isotype control (mouse IgG2b, BD PharMingen), then with CY 5-conjugated anti-mouse IgG (Jackson, West Grove, PA) diluted 1:400, and finally analyzed by flow cytometry using FACSCalibur (Becton Dickinson).

Results

mAb (5-15-1) reacted with epithelium of porcine small intestine

First, isolated porcine IECs were injected into BALB/c mice to generate mAbs capable of recognizing a unique cell surface molecule of IECs. A total of 10 mAbs were generated and tested for their reactivity using frozen sections prepared from porcine small intestine by immunohistochemical analysis. One of the mAbs, designated as mAb (5-15-1) with mouse IgG2b subclass, strongly reacted with the epithelium all the way from the villus (Fig. 1Aa) to the crypt (Fig. 1Ab) regions. Interestingly, the immunoreactivity was most strongly shown on the basolateral surface of the epithelium. An isotype control (Mouse IgG2b) did not react with the tissue sections of villus and crypt epithelium (Figs. 1Ac and d).

mAb (5-15-1) reacted with the 41–43 kDa protein of porcine small intestine when Western blot analysis was performed under nonreducing conditions

Inasmuch as 5-15-1 reacted with the epithelium of the porcine small intestine, the next logical step was to elucidate the molecular weight of the antigen recognized by 5-15-1. After immunoprecipitation of the small intestine with 5-15-1, a molecular mass of 41–43 kDa protein was detected by Western blot analysis under nonreducing conditions (Fig. 1Ba). Of course, this band was not detected in the negative control using the isotype control (mouse IgG2b) for immunoprecipitation or PBS instead of the lysate of the porcine small intestine (Fig. 1Ba). Nor was the band detected under reducing conditions (Fig. 1Bb). However, the band corresponding to the 5-15-1-specific antigen was detected by a G.P. Sensor, carbohydrate detection kit (Fig. 1Bc). These findings suggest that the surface antigen recognized by 5-15-1 belongs to a family of glycoproteins.

Immunoreactivity of mAb (5-15-1) with the other epithelial cells in mucosa-associated tissues

To further examine the immunoreactivity of 5-15-1 in several other mucosa-associated and systemic tissues, tissue sections were prepared from esophagus, stomach, duodenum, jejunum, ileum, appendix, colon, lung, spleen, and liver for immunohistological examination (Fig. 2). Among mucosa-associated epithelia, esophageal epithelial cells were stratified and flattened like skins cells and did not react with 5-15-1 (Fig. 2Aa). The lamina propria of the fundus ventriculi in the stomach is composed of fundic glands located under the epithelium and characterized by chief, pariental cells, and nebenzellen cells [32,33]. The newly developed mAb 5-15-1 reacted neither with the epithelial cells (Fig. 2Ab) nor with the chief, pariental, and nebenzellen cells in the fundic glands (Fig. 2Ac). When duodenum containing glandulae duodenales were examined, duodenum epithelial cells in the villus (Fig. 2Ad), crypt (Fig. 2Ae), and glands (Fig. 2Af) reacted with 5-15-1. The intestinal tract is composed of organized lymphoid structures known as gut-associated lymphoid tissue (GALT), an important inductive site for the mucosal immune system [2]. Therefore, sections of Peyer's patches (PPs) were examined for their reactivity with 5-15-1. Follicle-associated epithelium (FAE), one of the unique features of PPs,

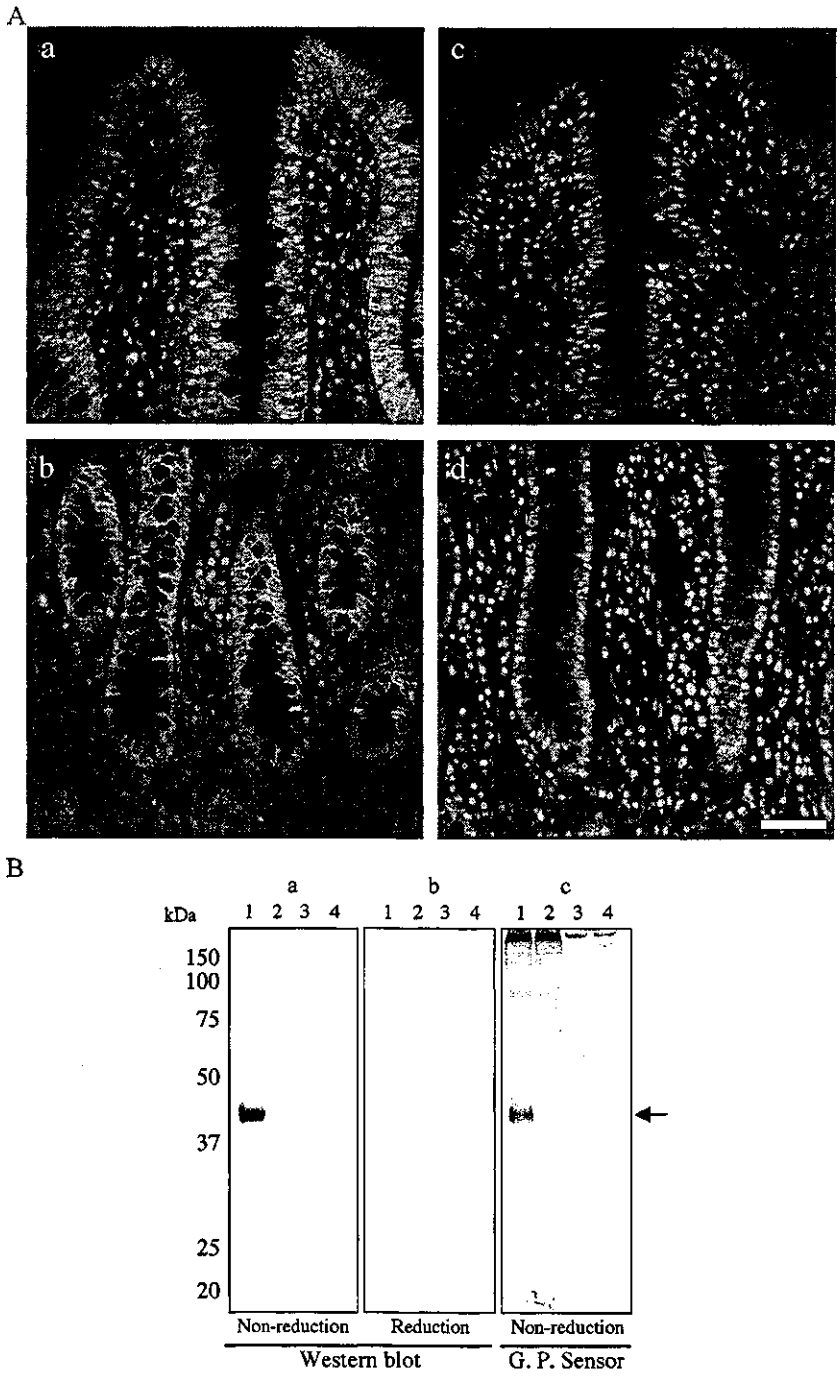

Fig. 1. Immunohistochemical and Western blot analyses of small intestine with mAb (5-15-1). Panel A shows tissue sections (5 μm) stained with the newly established mAb (5-15-1; mouse IgG2b) and with FITC-conjugated anti-mouse IgG followed by counterstaining with propidium iodate. (Aa and b) The immunoreactivity of 5-15-1; (Ac and d) the immunoreactivity of the isotype control. (Aa and c) The immunoreactivity in villus; (Ab and d) the immunoreactivity in the crypt. All of the intestinal epithelial cells (IECs) reacted with 5-15-1. Scale bar = 50 μm. Panel B shows the lysate of the small intestine (lanes 1 and 2) or the control (PBS, lanes 3 and 4), which was immunoprecipitated with 5-15-1 (lanes 1 and 3) or with an isotype control (mouse IgG2b, lanes 2 and 4) and then analyzed by Western blot. A protein measuring approximately 41–43 kDa was visible under nonreducing conditions (a) but not under reducing conditions (b). This 41–43 kDa protein was also detected under nonreducing conditions by G.P. Sensor (c).

exhibited strong immunoreactivity to 5-15-1 (Fig. 2Ag), while the leukocytes in PPs did not (Fig. 2Ah). Both the large (Fig. 2Ai) and the small (Figs. 1Aa and b) intestinal epithelium strongly reacted to 5-15-1, as did some alveolar cells and all of the epithelial cells of the bronchus in the lung (Fig. 2Aj). However, neither hepatocytes (Fig. 2Ak) nor splenocytes (Fig. 2Al) showed reactivity to 5-15-1. Looked at collectively, these results suggest that 5-15-1 specifically reacted with mucosal epithelia composed of columnar epithelial cells.

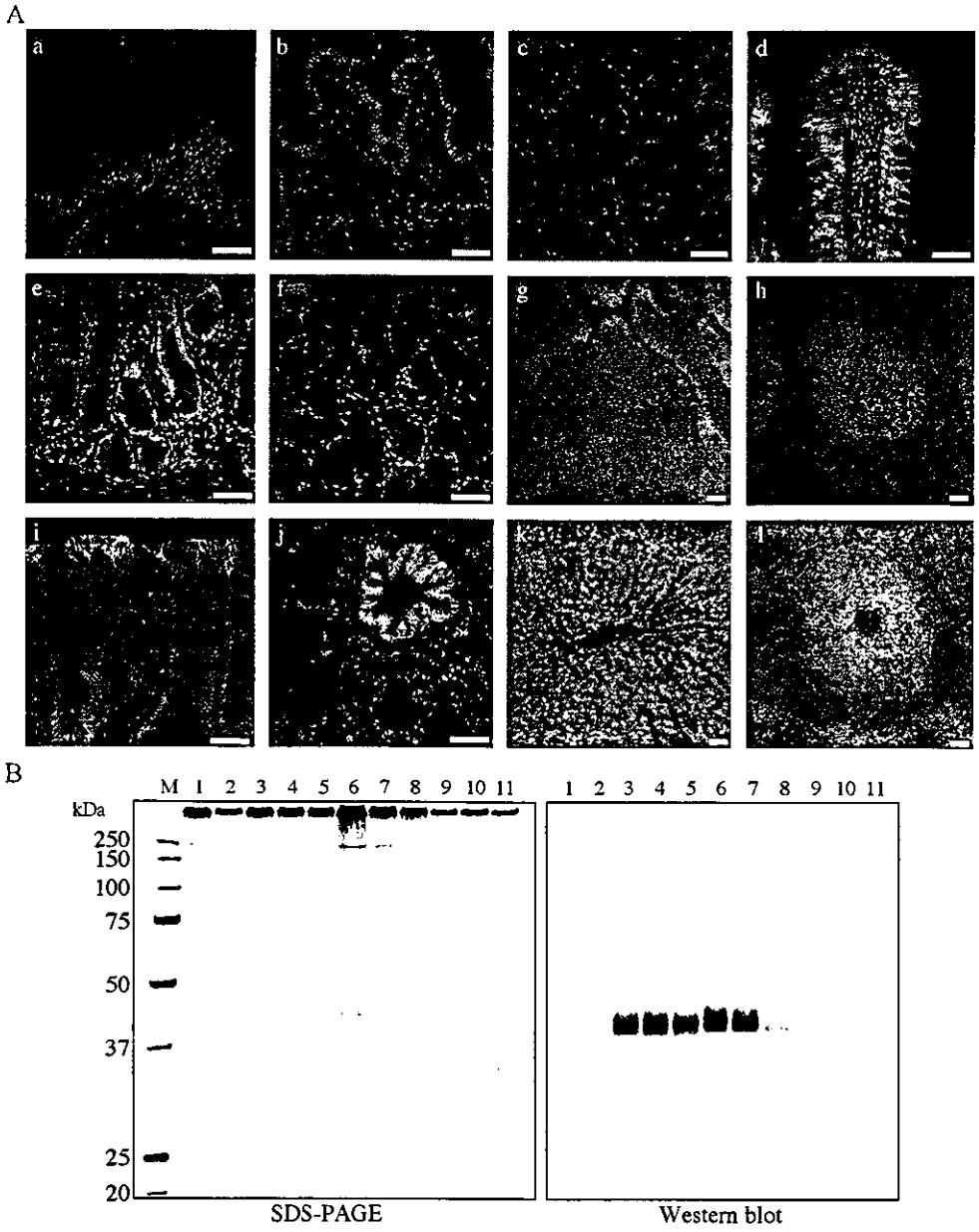

Fig. 2. Immunohistochemical and Western blot analyses of different mucosa-associated tissues with mAb (5-15-1). Panel A shows tissue sections (5 μm) stained with 5-15-1 and FITC-conjugated anti-mouse IgG followed by counterstaining with propidium iodate. Almost all of the epithelial tissues, with the exception of the esophagus and stomach, reacted with 5-15-1. (a) Esophageal epithelium, (b) stomach epithelium, (c) fundic gland in stomach, (d) epithelium in duodenum, (e) crypt in duodenum, (f) gloandulae deodenales in duodenum, (g) follicle-associated epithelium (FAE) in Peyer's patch, (h) lymphoid follicle in Peyer's patch, (i) epithelium in colon, (j) epithelium in lung, (k) hepatocyte in liver, (l) splenocyte in spleen. Scale bar = 50 μm. Panel B shows the results obtained when lysates (5 mg) of different mucosa-associated tissues were immunoprecipitated with 5-15-1 (10 μg/ml) and then analyzed by Western blot. The left panel shows the data obtained using SDS-PAGE, the right panel that obtained using Western blot. A protein with a molecular mass of 41–43 kDa was visible in the duodenum, jejunum, ileum, appendix, colon, and lung but not in the esophagus, stomach, liver, and spleen under nonreducing conditions. (1) Esophagus, (2) stomach, (3) duodenum, (4) jejunum, (5) ileum, (6) appendix, (7) colon, (8) lung, (9) liver, (10) spleen, (11) mAb alone.

Immunoprecipitation and Western blot analysis revealed the presence of the 41–43 kDa protein in all mucosa-associated tissues except the esophagus and stomach

We next used immunoprecipitation and Western blot analyses to confirm our immunohistochemical findings regarding the tissue specificity of 5-15-1 for several mucosal-associated epithelia. Lysates prepared from different mucosa-associated and systemic tissues were precipitated with 5-15-1 and then analyzed by SDS-PAGE and Western blot analyses under nonreducing conditions. The antigen corresponding to a molecular mass of 41–43 kDa was detected in the duodenum, jejunum, ileum, appendix, colon, and lung, but not in the esophagus, stomach, spleen, and liver. The results obtained by SDS-PAGE and

Western blot analyses of these different tissue extracts (Fig. 2B) confirmed the data generated by the immunohistochemical analysis (Fig. 2A). Further, the data analyzed by Western blot revealed that the expression level of the antigen was roughly equal in the duodenum, jejunum, ileum, appendix, and colon, but considerably lower in the lung (Fig. 2B).

IELs but not splenocytes and PBMCs reacted with 5-15-1

Since 5-15-1 specifically reacted with the glycoprotein antigen (41–43 kDa) associated with the intestinal epithelium, we sought to determine whether a similar protein is also expressed by neighboring IELs. Flow cytometry was used to determine the immunoreactivity to 5-15-1 of IELs and IECs isolated from porcine small intestine. Splenocytes and PBMCs isolated from the same pig served as controls. First, IELs were separated from IECs on the basis of cell size and granularity (Fig. 3a). A fraction of IELs was greater than 98% positive for CD45, while the IECs fraction did not contain any CD45-positive cells (data not shown). As expected from the findings discussed above (Fig. 1A), freshly isolated IECs were positive for 5-15-1 (Fig. 3b). Interestingly, however, IELs also reacted with 5-15-1 (Fig. 3c). When the mean fluorescence intensity of the two fractions was compared, that of IELs was weaker than that of IECs (Fig. 3f). Splenocytes (Fig. 3d) and PBMCs (Fig. 3e) did not react with 5-15-1. These findings demonstrate that the glycoprotein, which reacted with 5-15-1, was also expressed by IELs in addition to IECs in the intestinal epithelium.

MALDI-TOF-MS and tandem MS analysis of 5-15-1 reactive 41–43 kDa protein resulted in the identification of a porcine homologue of the human pan-carcinoma antigen epithelial glycoprotein (EGP), or alias epithelial adhesion molecule (Ep-CAM)

Since it was expressed by both IECs and IELs, we sought to identify the exact nature of the 41–43 kDa protein recognized by 5-15-1. The antigen was first purified from small intestine lysates using affinity chromatography with 5-15-1 and then separated out using SDS-PAGE (Fig. 4A). When the 41–43 kDa protein was analyzed by MALDI-TOF-MS analysis after tryptic digestion, several major peaks were identified (Fig. 4B). Four major peaks (asterisks) were randomly selected and further analyzed by tandem MS. The amino acid sequence of one of the peaks (arrow in Fig. 4B) was identified as IADVAYYFEK (Fig. 4C). A search of the "MASCOT" database confirmed this sequence as human pan-carcinoma antigen epithelial glycoprotein (EGP), or alias epithelial adhesion molecule (Ep-CAM). In contrast, the other three peaks were identified as actin (data not shown).

Cloning of porcine Ep-CAM

To formally prove that the antigen of 5-15-1 is a porcine homologue of human Ep-CAM, the next logical step was to clone and sequence the porcine Ep-CAM. Fig. 5 shows both the sequence including the initiation and stop codon and the predicted amino acid sequence.

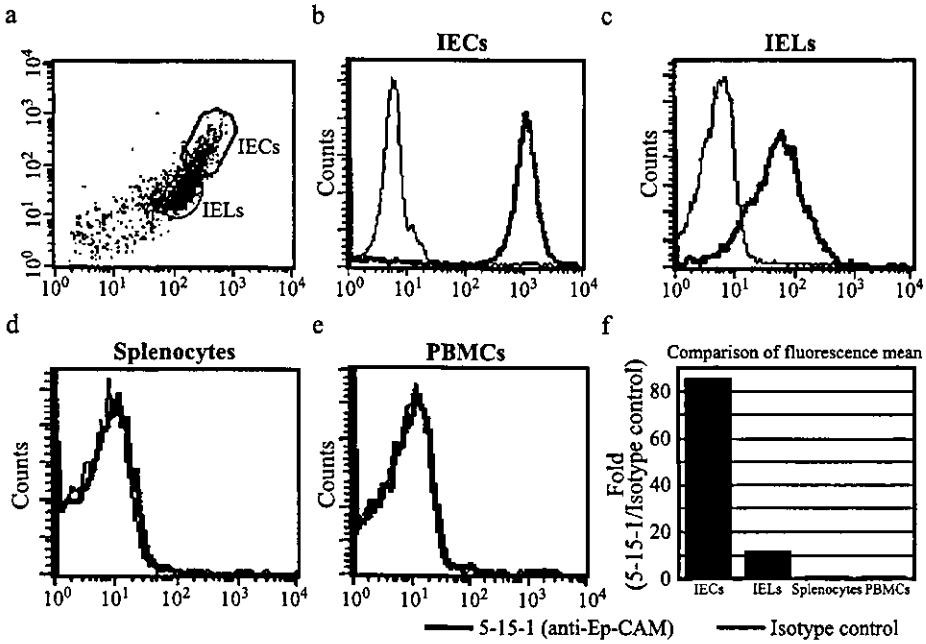

Fig. 3. Immunoreactivity of mAb (5-15-1) against IECs, IELs, splenocytes, and PBMCs. Isolated IECs, IELs, splenocytes, and PBMCs were stained with mAb (5-15-1) and FITC-conjugated anti-mouse IgG and then analyzed using flow cytometry. IECs and IELs were separated based on cell size and granularity (a). IECs (b) and IELs (c), but not splenocytes (d), and PBMCs (e) reacted with 5-15-1. The fluorescence mean intensity was also examined (f).

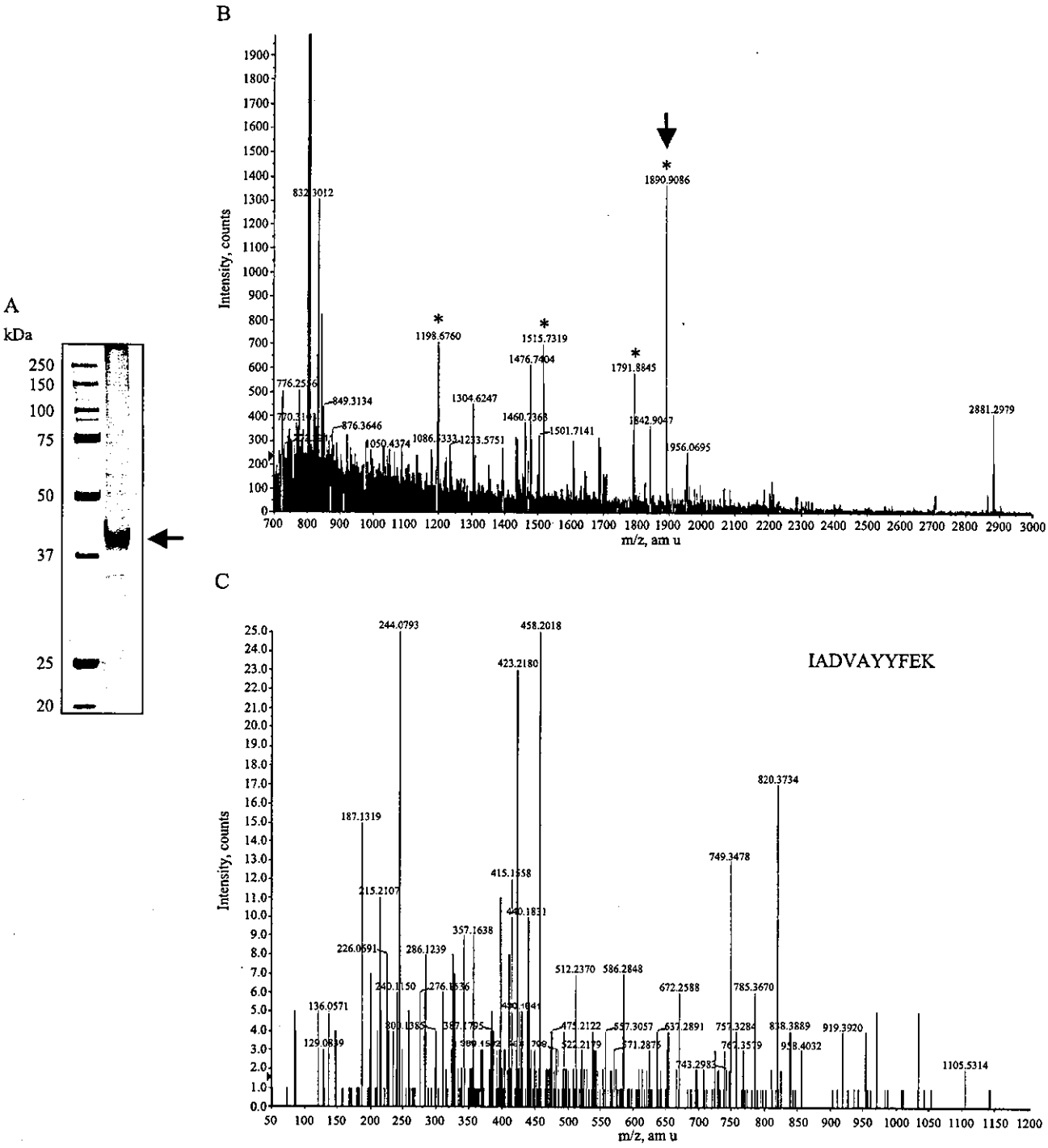

Fig. 4. Identification of the antigen purified by affinity chromatography with 5-15-1. Panel A shows the SDS-PAGE analysis of the antigen purified by affinity chromatography with 5-15-1. A protein with a molecular mass of 41–43 kDa was analyzed by MALDI-TOF-MS and tandem MS analysis. Panel B shows the MALDI-TOF-MS spectrum of the 41–43 kDa antigen digested by trypsin. Four major peaks (asterisks) were further analyzed by tandem MS. Panel C shows that the tandem MS spectrum of one of the four peaks (arrow in Panel B) was sequenced and identified as "IADVAYYFEK."

As one might expect, the cloned sequence contains tandem MS-identified "IADVAYYFEK." The sequence data were then registered with GenBank (Accession number: AB161197). The cDNA contains an open reading frame (ORF) of 945 bp and encodes for 314 amino acids. Compared with human, mouse, and rat sequences, the porcine Ep-CAM displays 82.9%, 71.3%, and 71.8% homology at the nucleotide level and 82.8%, 78.1%, and 76.8% homology at the amino acid level, respectively (Fig. 5). Porcine Ep-CAM is a type-I transmembrane protein of which the first 23 amino acids are putatively the signal sequence. A 242 amino acid, cystein-rich extracellular

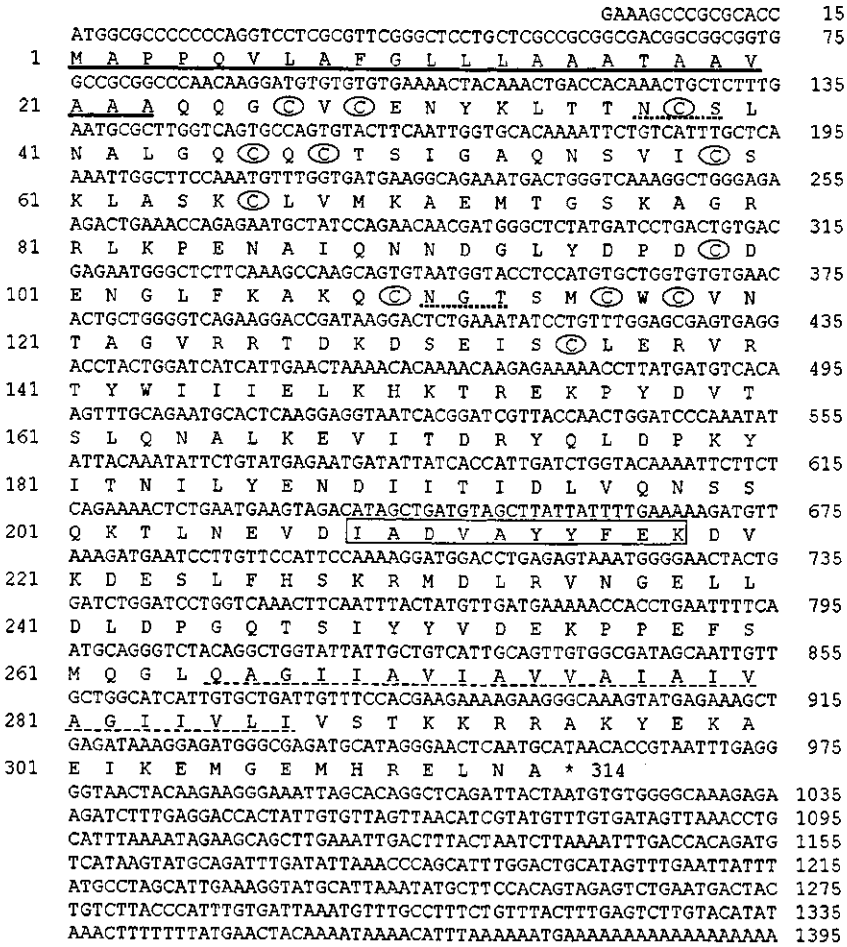

Fig. 5. DNA and amino acid sequence of porcine Ep-CAM. An open reading frame predicts a protein of 314 amino acids. A putative signal sequence (first bolded underline), 12 cysteine residues (circles), two potential N-linked glycosylation sites (bold and dotted underline), and one transmembrane domain (dotted underline) are indicated. The amino acid sequence matched that of the molecule identified by MALDI-TOF-MS and tandem MS analyses was shown in the box.

domain is followed by a 23 amino acid hydrophobic transmembrane domain and a 26 amino acid highly charged intracellular domain. There are two potential N-linked glycosylation sites in the extracellular domain. These molecular characteristics are very similar to those seen in human, mouse, and rat Ep-CAM [28–30].

mAb (5-15-1) reacted COS-7 transfected with the cDNA of porcine Ep-CAM

To directly confirm that the antigen of 5-15-1 is porcine Ep-CAM, we generated COS-7 cells transfecting the cDNA of porcine Ep-CAM. For the transfection, we purposely used the pIRES2-EGFP vector system since it is capable, by merit of its containing the IRES sequence, of expressing enhanced GFP (EGFP) and porcine Ep-CAM under one mRNA transcript [34]. The expression plasmid map (pIRES2-EGFP-pEp-CAM) is shown in Fig. 6A. When successfully transfected with pIRES2-EGFP-pEp-CAM, COS-7 cells expressed EGFP and Ep-CAM that could be recognized by 5-15-1 (Fig. 6B). In contrast, COS-7 transfected with an empty vector (pIRES2-EGFP) expressed EGFP but did not react with 5-15-1. These findings demonstrate that 5-15-1 possesses specificity for porcine Ep-CAM.

Expression of Ep-CAM by both IECs and IELs

To definitively prove that Ep-CAM is expressed by both the IECs and IELs of the intestinal epithelium, we performed an immunohistochemical analysis of the intestinal epithelium using FITC-conjugated 5-15-1 specific for Ep-CAM and rhodamine-coupled anti-porcine CD45 mAb together with DAPI counterstaining. The immunohistochemical analysis revealed that Ep-CAM was expressed by IECs and IELs. It is important to note that the expression of Ep-CAM and CD45 were colocalized on the cell surface of IELs (arrowhead in Fig. 7A). In contrast, CD45-positive lymphocytes located in the lamina propria region did not express Ep-CAM (arrow in Fig. 7A). CD45-positive splenocytes also did not react with Ep-CAM-specific mAb 5-15-1 (Fig. 7B). These findings